Dielectric rod waveguides and antennas for low THz frequencies

Dmitri V. Lioubtchenko

CENTERA Laboratories, Institute of High Pressure Physics, PAS
ul. Sokołowska 29/37, 01-142, Warsaw, Poland
Department of Micro and Nanosystems, KTH Royal Institute of Technology
Malvinas väg 10, SE-100 44 Stockholm, Sweden

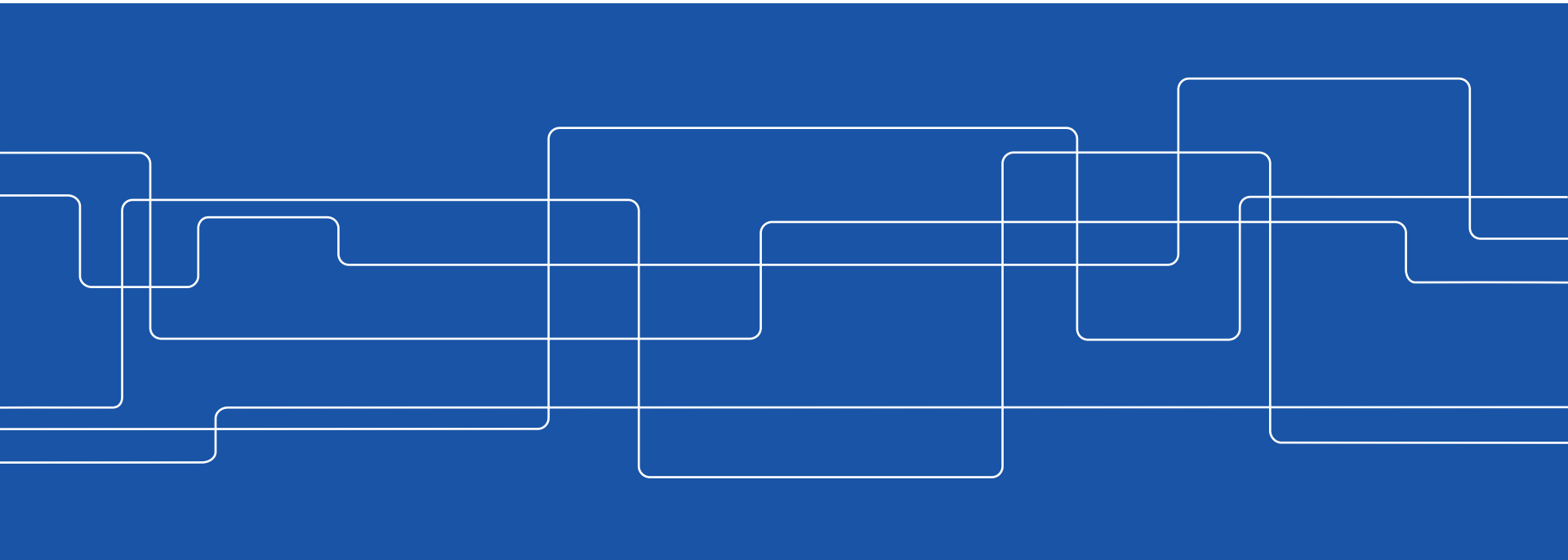

Waveguides used at 0.1-1 THz

- Metal waveguides
  rectangular and circular
- Dielectric waveguides
  rectangular and circular
- Microstrip line

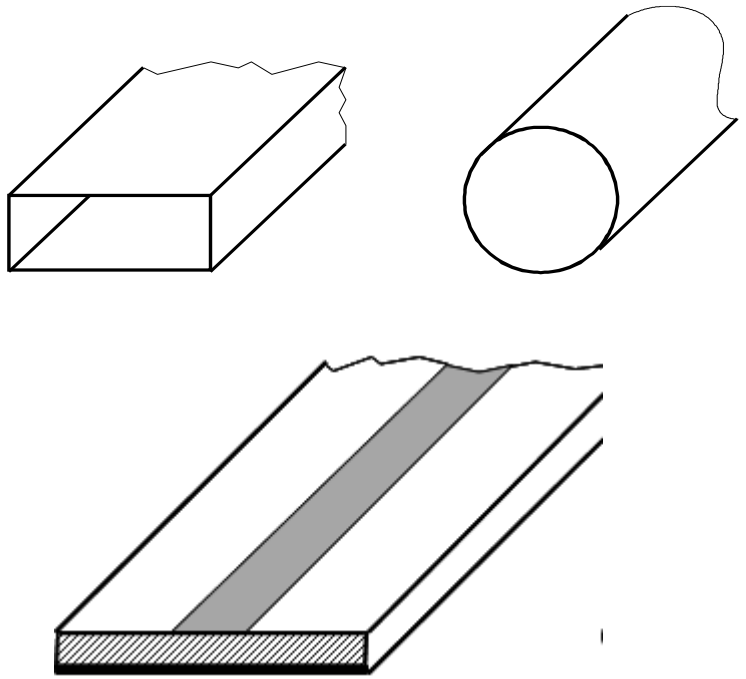

D. Lioubtchenko, S. Tretyakov, S. Dudorov, Millimeter-Wave Waveguides, Kluwer Academic Publishers, The Netherlands, 2003

Waveguides used at 0.1-1 THz

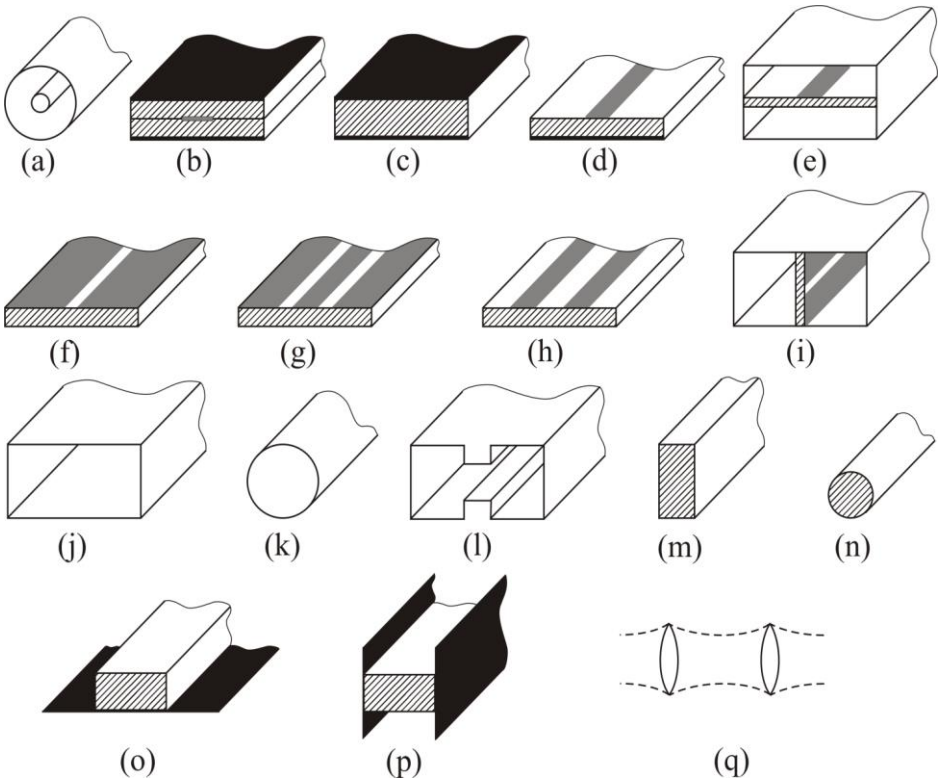

(a) coaxial line
(b) stripline,
(c) parallel plate waveguide,
(d) microstrip line,
(e) suspended stripline,
(f) slotline,
(g) coplanar waveguide,
(h) coplanar stripline,
(i) fin line,
(j) rectangular hollow metal waveguide,
(k) circular hollow metal waveguide,
(l) groove guide,
(m) rectangular dielectric rod waveguide,
(n) circular dielectric rod waveguide,
(o) image guide,
(p) H-guide,
(q) quasioptical waveguide

D. Lioubtchenko, S. Tretyakov, S. Dudorov, Millimeter-Wave Waveguides, Kluwer Academic Publishers, The Netherlands, 2003

Metal waveguides

VDI Designation	Internal Dimensions (µm)		Cut-off frequency (GHz)	Suggested min. frequency (GHz)	Suggested max. frequency (GHz)	Calculated Loss (dB/cm) for Au *		Alternate Designations	
	Width	Height				At min. frequency	At max. frequency		
WR-15	3759	1880	39.9	50	75	0.022	0.015	V	-
WR-12	3099	1549	48.4	60	90	0.030	0.020	E	-
WR-10	2540	1270	59.01	75	110	0.039	0.027	W	-
WR-8.0	2032	1016	73.77	90	140	0.059	0.038	F	WR-8
WR-6.5	1651	825.5	90.79	110	170	0.081	0.052	D	WR-6
WR-5.1	1295	647.5	115.75	140	220	0.12	0.074	G	WR-5
WR-4.3	1092	546	137.27	170	260	0.14	0.1	-	WR-4
WR-3.4	864	432	173.49	220	330	0.2	0.14	-	WR-3
WM-710 (WR-2.8)	710	355	211.12	260	400	0.28	0.18	-	-
WM-570 (WR-2.2)	570	285	262.98	330	500	0.37	0.25	-	-
WM-470 (WR-1.9)	470	235	318.93	400	600	0.5	0.34	-	-
WM-380 (WR-1.5)	380	190	394.46	500	750	0.67	0.47	-	-
WM-310 (WR-1.2)	310	155	483.54	600	900	0.95	0.64	-	-
WM-250 (WR-1.0)	250	125	599.58	750	1100	1.3	0.88	-	-
WM-200 (WR-0.8)	200	100	749.48	900	1400	2	1.2	-	-
WM-164 (WR-0.65)	164	82	914	1100	1700	2.6	1.7	-	-
WM-130 (WR-0.51)	130	65	1153	1400	2200	3.7	2.3	-	-
WM-106 (WR-0.43)	106	53	1414.1	1700	2600	5.1	3.2	-	-
WM-86 (WR-0.34)	86	43	1743	2200	3300	6.3	4.3	-	-

* Waveguide loss calculated according to IEEE P1785.1

Virginia Diodes, Inc.
www.vadiodes.com

Losses in waveguides

- Conductor loss $\frac{1}{2}\int \left|\bar{J}_s\right|^2 R_s dc$, in which $\bar{J}_s = \bar{n} \times \bar{H}$

  and $R_s \cong \sqrt{\omega \mu_0 / 2\sigma_m}$ (surface resistance)

- Conductor loss for TE_{10} mode

$$\alpha_{cTE10} = \frac{R_s}{\eta\sqrt{1-(\lambda/2a)^2}}\left(\frac{1}{b}+\frac{\lambda^2}{2a^3}\right) \Rightarrow \alpha_{cTE10} \sim f^{\frac{3}{2}}$$

~f

constant

$$\alpha_d = \frac{\pi}{\lambda_d}\frac{\tan\delta}{\sqrt{1-(f_c/f)^2}} \Rightarrow \alpha_d \sim f$$

constant

The total attenuation constant

$$\alpha = \alpha_c + \alpha_d$$

D. Lioubtchenko, S. Tretyakov, S. Dudorov, Millimeter-Wave Waveguides, Kluwer Academic Publishers, The Netherlands, 2003

Types of rectangular DRW

Main types of dielectric waveguide
a) open waveguide,
b) image waveguide,
c) isolated image waveguide,
d) layered ribbon dielectric waveguide,
e) and f) other types.

b-e) – mm-wave integrated circuits based on DRW

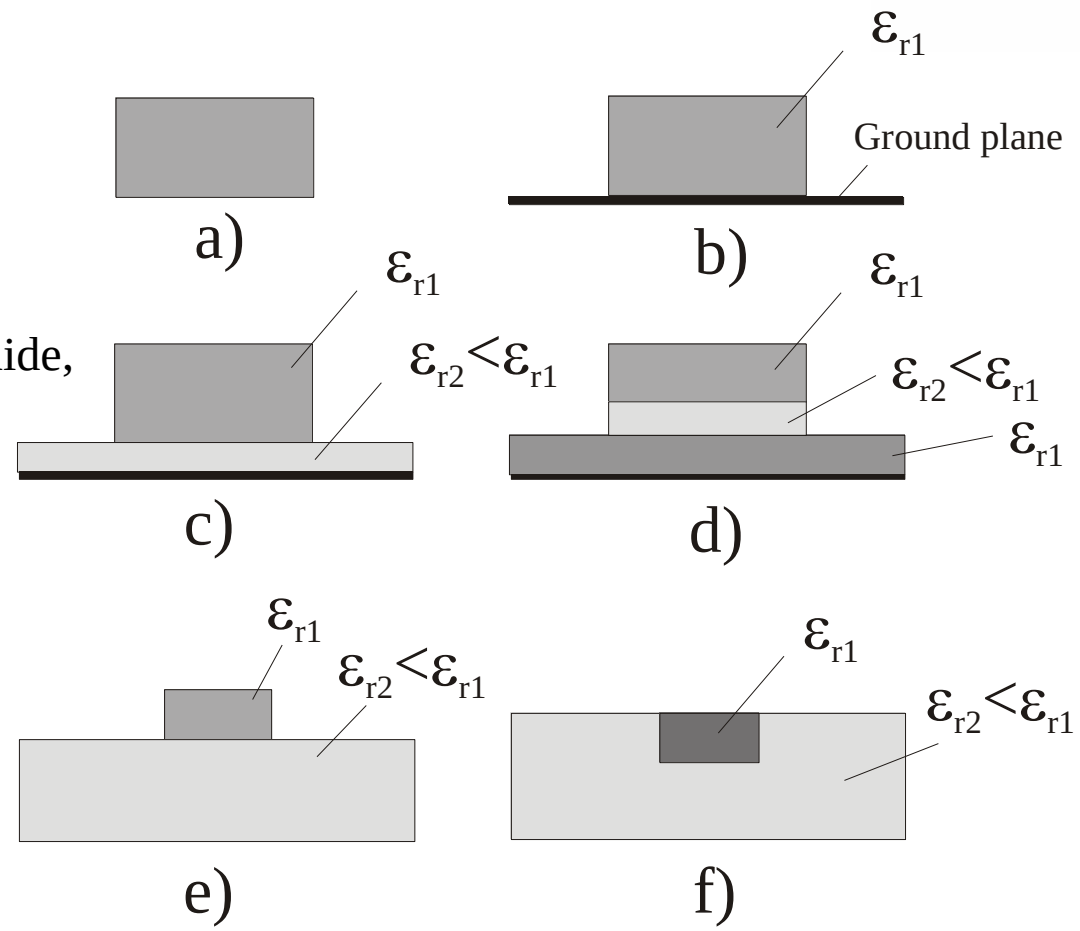

Open DRWs

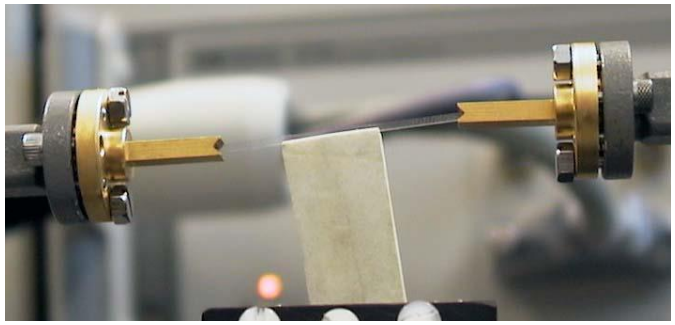

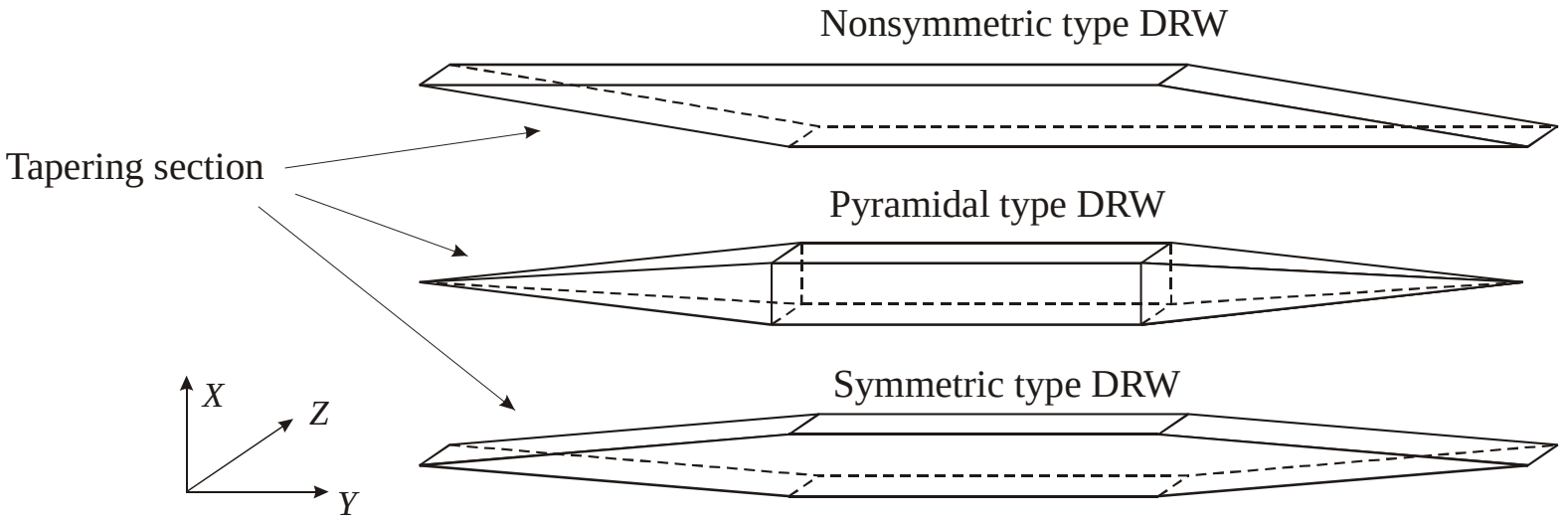

D. Lioubtchenko, S. Tretyakov, S. Dudorov, Millimeter-Wave Waveguides, Kluwer Academic Publishers, The Netherlands, 2003

Fabrication of DRW

First DRWs were made of low dielectric constant materials.

High permittivity dielectrics or semiconductors will have smaller cross sections.

The rectangular cross-section to prevent it is to design the waveguide so that different polarizations have different propagation constants.

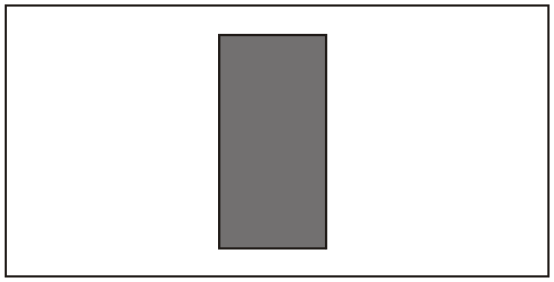

The field in vertical direction in the metal waveguide is concentrated stronger than in the horizontal direction. To get good matching we have to have the field distribution in the dielectric waveguide as close as possible to that in the metal waveguide.

Dielectric properties of materials (at 140 GHz)

Materials	**Si**	**Diamond**	**GaAs**	**BN**	**Quartz**	**Teflon**	**Ceramic (Al_2O_3)**	**AlN**	**Ferrite**	**Sapphire**
ε	11.6-11.8	5.6644	10.9-13.03	3.179	4.44-4.64	1.96-2	10.5	7.7-9.5	13.32(NiZn) 15.6 (Li) 15.05 (FeY)	9.39, 11.56
$\tan\delta x10^{-4}$	0.01	0.08	3	8-15	0.9-1.8	3-4	2.7-3.2	4.5	1.24-7.5	1.1 – 2.1

D. Lioubtchenko, S. Tretyakov, S. Dudorov, Millimeter-Wave Waveguides, Kluwer Academic Publishers, The Netherlands, 2003

Dimensions of DRW

In the case of very small dimensions we have very small losses but bad wave guiding properties and difficulties with matching. Another way to decrease the propagation losses is to increase the dimensions. In that case we are limited by the possibility to get multimode regime.

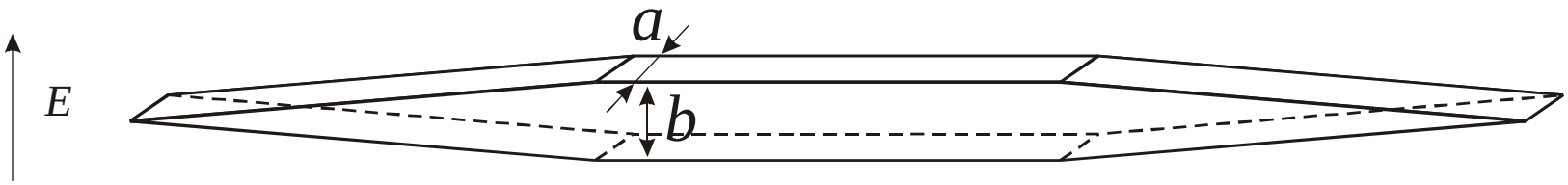

Ratio of a / b = 0.5 and $k_0 b$ = 1.7 – 1.9, where $k_0 = \frac{2\pi}{\lambda_0}$ – propagation constant in vacuum;

λ_0 – central wavelength of the operation frequency range in vacuum

Propagation constant calculation

Circular dielectric waveguides can be solved in terms of the Bessel functions.

In case of the rectangular cross section no closed-form solution exists.

However, in the case of the open rectangular dielectric waveguide, it occurred to be impossible, and the propagating modes are referred as **hybrid modes**.

Lets call the propagating mode E^{y}_{mn}, if its electric field is polarized mainly along the *y*-direction, and E^{x}_{mn}, if the strongest electrical field component points along the *x*-direction according.

Marcatili's method

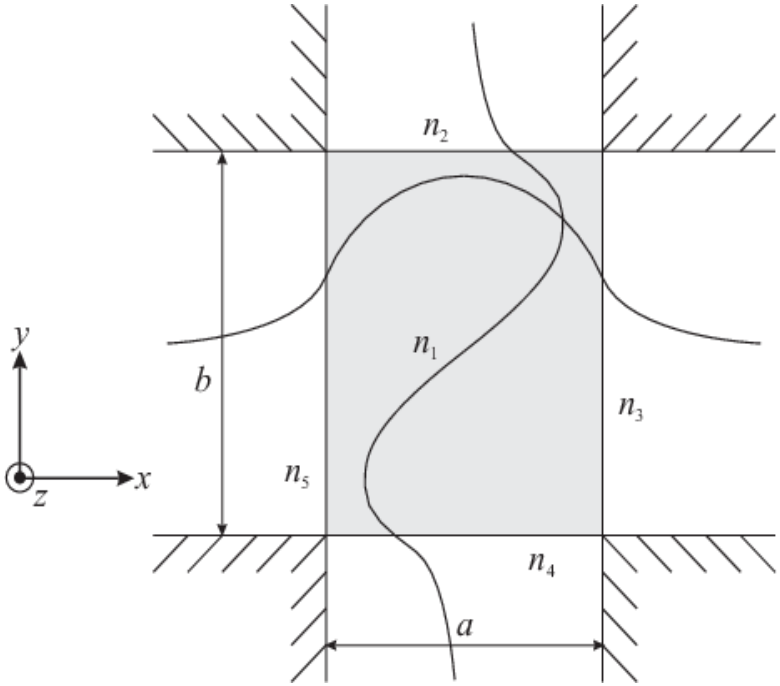

- Developed for low ratios between the core permittivity and that of the cladding region (slightly more than 1).
- The complete cross section area is divided into five regions.
- The fields in the shadowed regions are not considered.
- In all the other regions, the fields are assumed to be approximately (co)sinusoidally distributed inside the waveguide and decaying exponentially outside.

S.N. Dudorov, D.V. Lioubtchenko, A.V. Räisänen. "Modification of Marcatili's method for the calculation of anisotropic rectangular dielectric waveguides". IEEE Transactions on Microwave Theory and Techniques vol. 50, no. 6, 2002 pp.1640-1642

Goell's method

Instead of expanding the field distribution in sinusoidal functions, Goell proposed to use the following approach: the electric and magnetic fields inside the core of the dielectric waveguide as

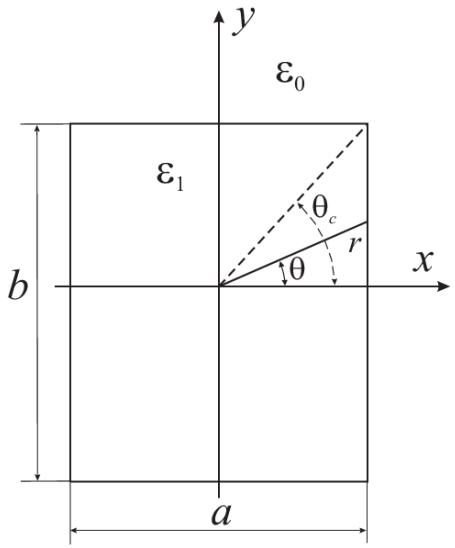

E and H fields inside the core

$$E_{z1} = \sum_{n=0}^{+\infty} a_n J_n(\beta_t r)\sin(n\theta + \phi_n)\exp(-jk_z z + j\omega t)$$

$$H_{z1} = \sum_{n=0}^{+\infty} b_n J_n(\beta_t r)\sin(n\theta + \psi_n)\exp(-jk_z z + j\omega t)$$

E and H fields outside the core

$$E_{z0} = \sum_{n=0}^{+\infty} c_n K_n(qr)\sin(n\theta + \phi_n)\exp(-jk_z z + j\omega t)$$

$$H_{z0} = \sum_{n=0}^{+\infty} d_n K_n(qr)\sin(n\theta + \psi_n)\exp(-jk_z z + j\omega t)$$

$$\beta_t = \sqrt{k_1^2 - k_z^2}$$

$$q = \sqrt{k_z^2 - k_0^2}$$

the transverse propagation constants inside and outside of the dielectric rod

Modes in the DRW

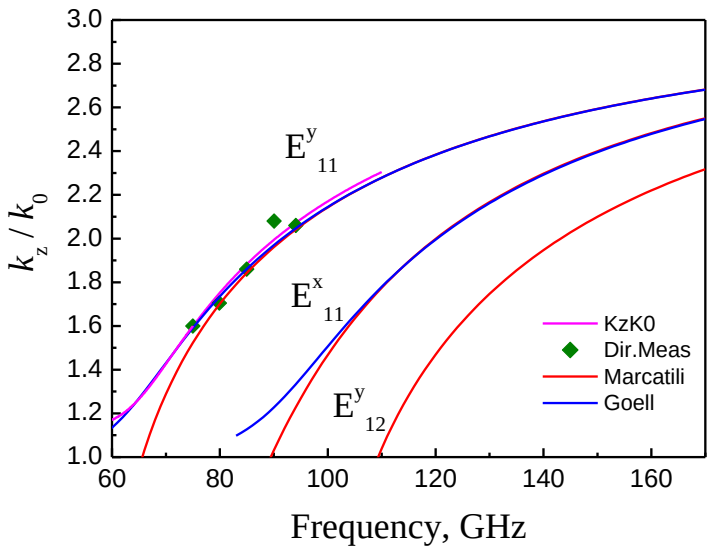

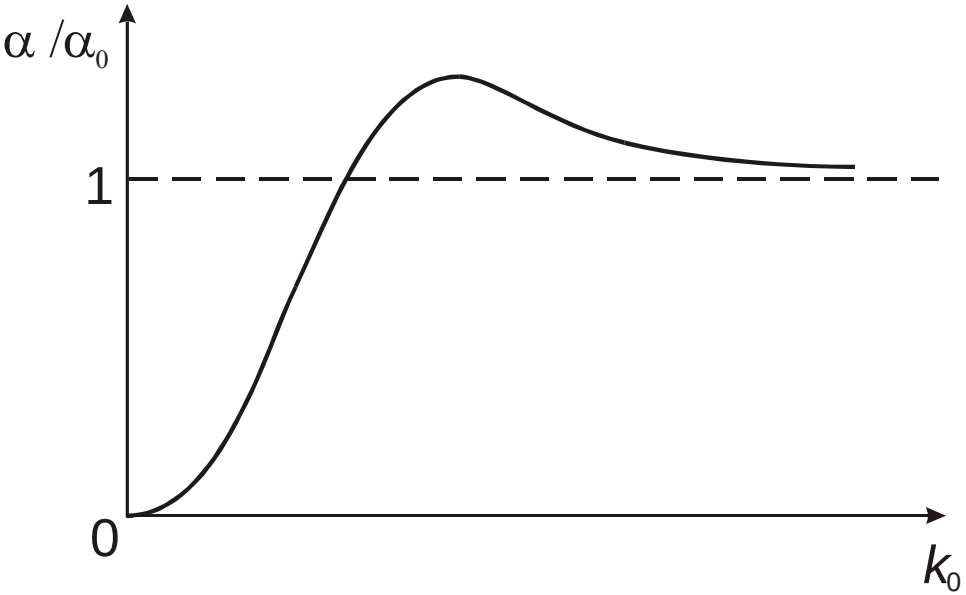

Schematic dispersion characteristic of DRW and dependence of loss factor $\frac{\alpha}{\alpha_0}$ on frequency.

k_0 is the wave number in vacuum, $\alpha_0 = \frac{1}{2} kn \tan\delta$ is the attenuation constant of an infinite medium,

filled with the same dielectric, *n* is the refractive index of the DRW.

S.N. Dudorov, D.V. Lioubtchenko, J.A. Mallat, A.V. Räisänen. "Modified Goell's method for the calculation of uniaxial anisotropic rectangular dielectric waveguides". Microwave and Optical Technology Letters vol. 32, no. 5, 2002, pp.373-376

Fields in DRW

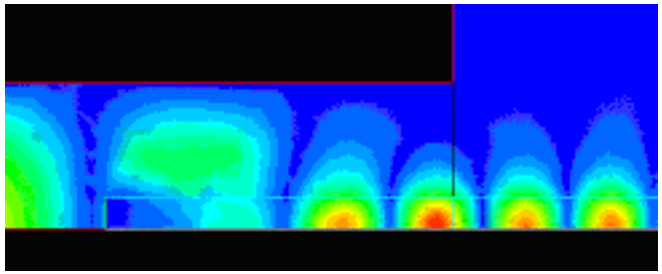

H-plane (*xy*), E-field magnitude at 93 MHz.

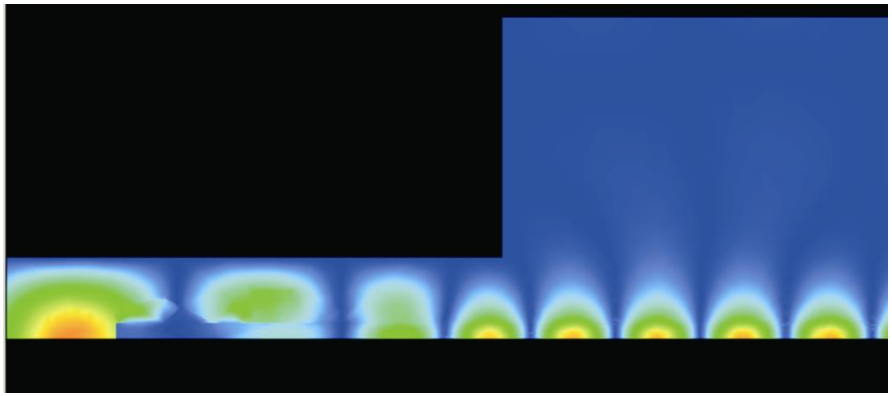

H-plane (*xy*), E-field magnitude at 75 MHz.

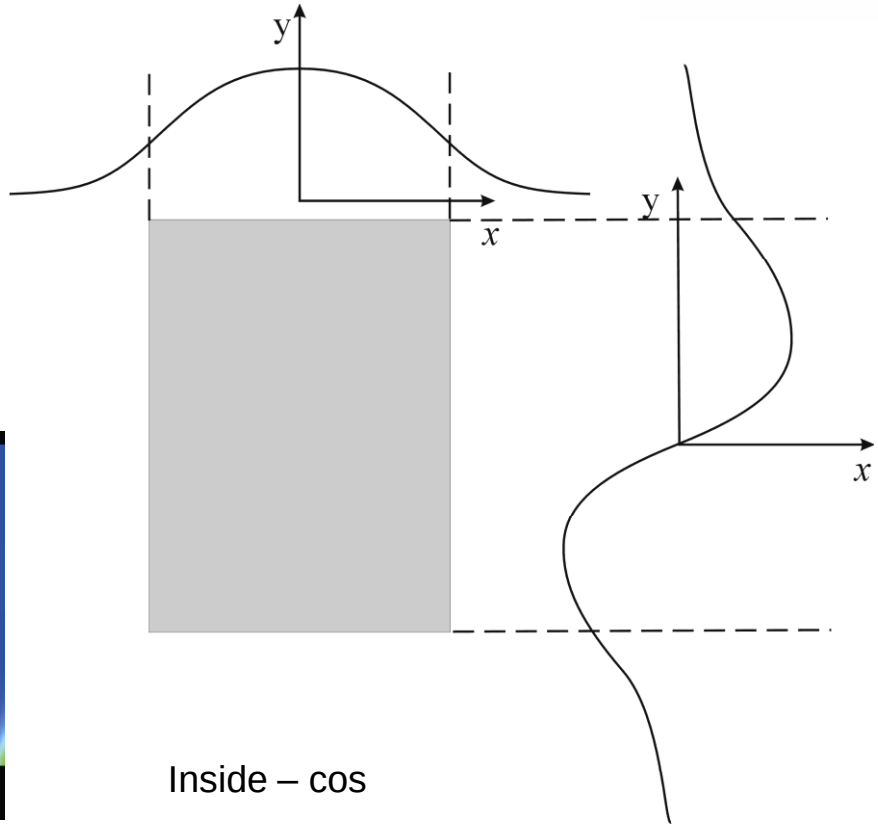

Inside – cos

Outside – exp

D. Lioubtchenko, S. Tretyakov, S. Dudorov, Millimeter-Wave Waveguides, Kluwer Academic Publishers, The Netherlands, 2003

Field distribution in dielectric rod waveguide

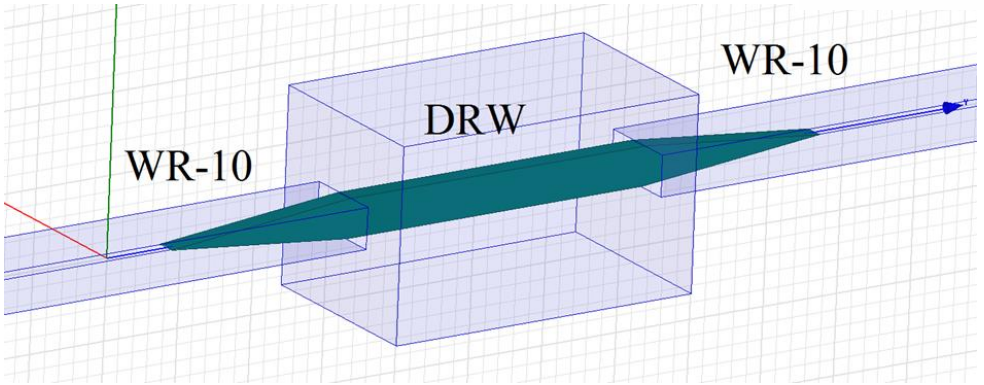

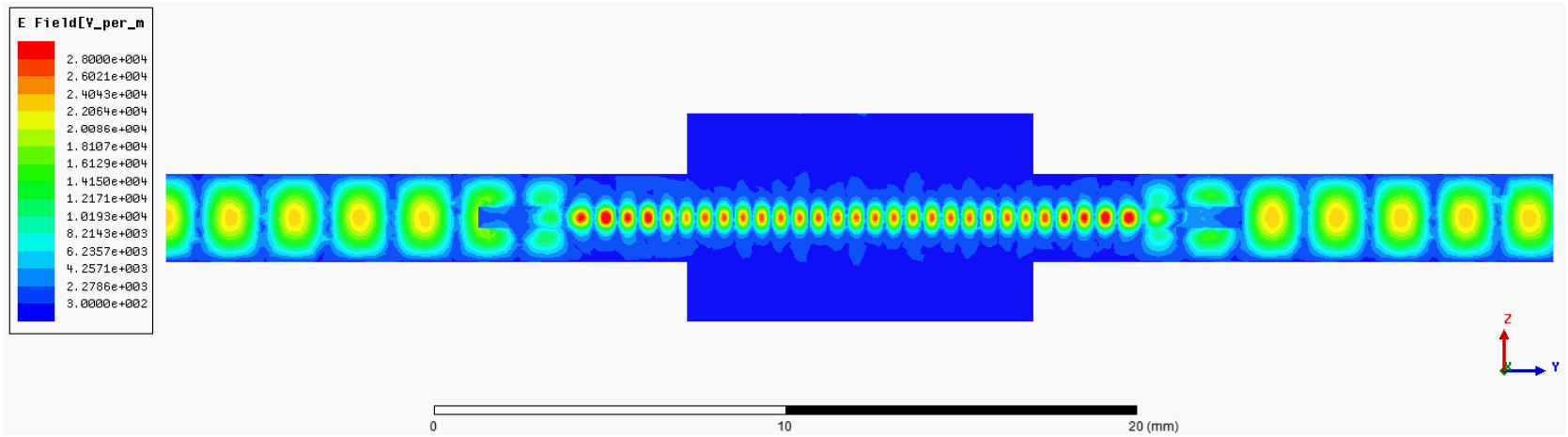

HFSS simulations of different DRW cross-sections

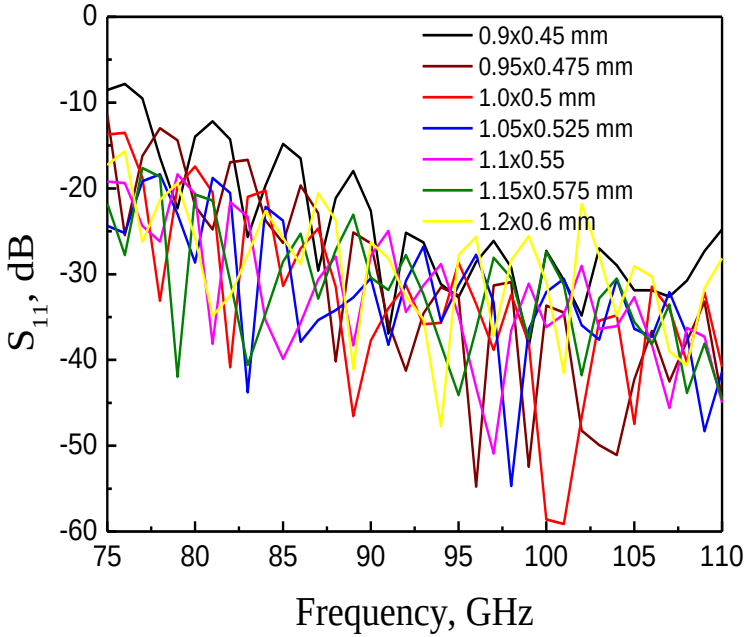

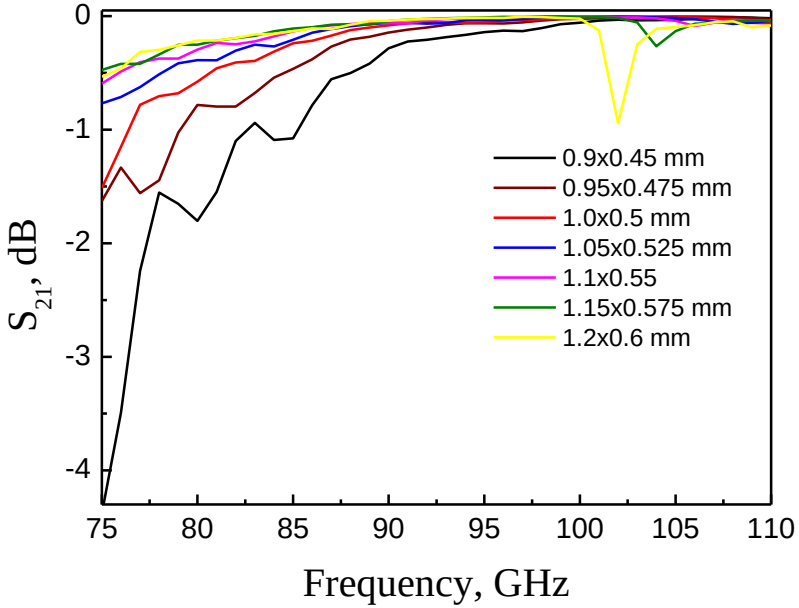

D. Lioubtchenko, S. Tretyakov, S. Dudorov, Millimeter-Wave Waveguides, Kluwer Academic Publishers, The Netherlands, 2003

Sapphire DRW

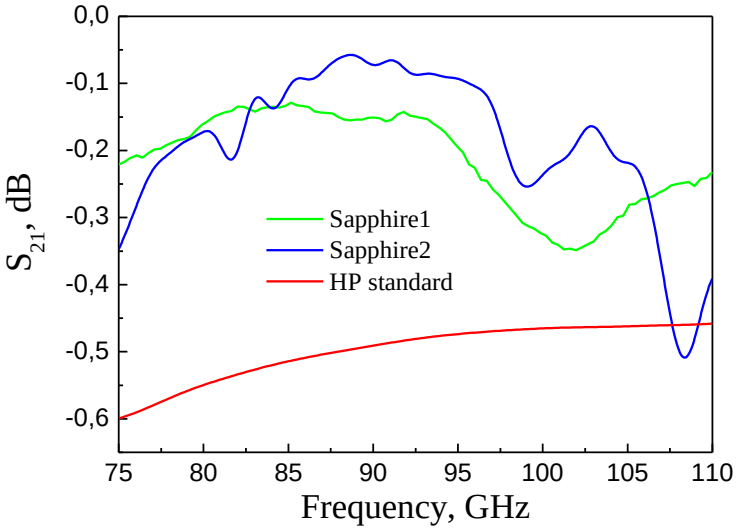

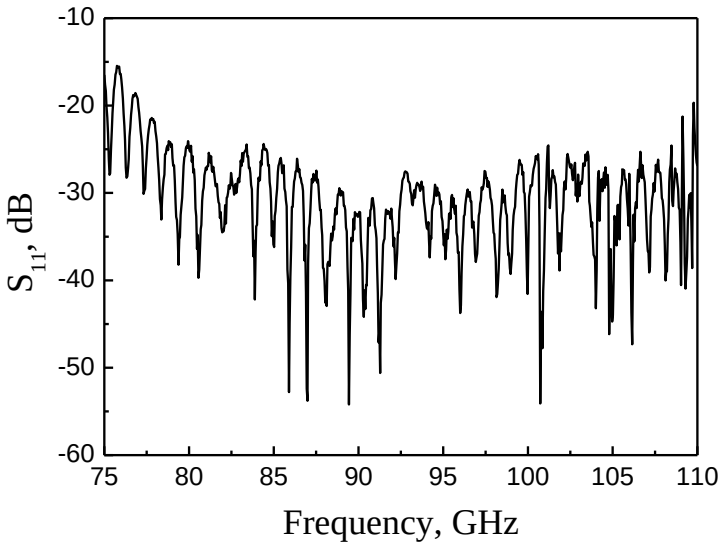

D. Lioubtchenko, S. Dudorov, J. Mallat, J. Tuovinen, A.V. Räisänen. “Low loss sapphire waveguides for 75-110 GHz frequency range” IEEE Microwave and Wireless Components Letters vol. 11, no. 6, 2001, pp. 252-254.

Non-radiating dielectric waveguide

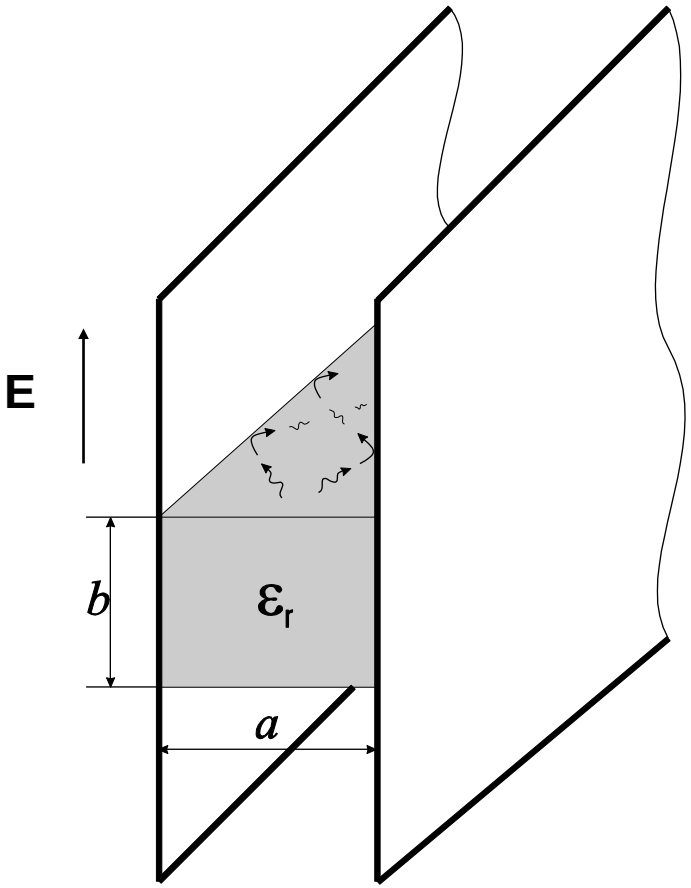

It is similar to a metal waveguide filled with dielectric with wider walls removed and narrower walls enlarged.

Thus the ohmic losses in metal are significantly reduced.

$$\frac{a}{\lambda} \approx 0.45; \quad \sqrt{\varepsilon_r - 1}\frac{b}{\lambda} \approx 0.4...0.6$$

The radiation can be almost completely suppressed and the design of directional couplers, power dividers, circulators, etc. can be considerable simplified.

Operational mode – a combination of two TM modes of dielectric slab waveguide reflecting from metal plates.

Operation frequency region increases if to increase the ε

Difficult to integrate three-terminal devices (transistors)

Directional coupler

(Aperture coupling configuration)

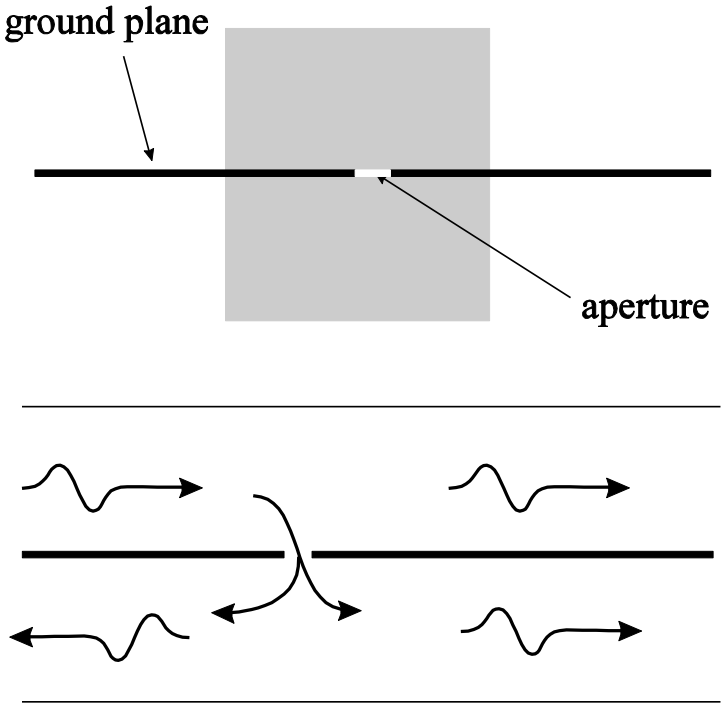

Two DRW separated by a metal hole

Directional coupler based on DRW

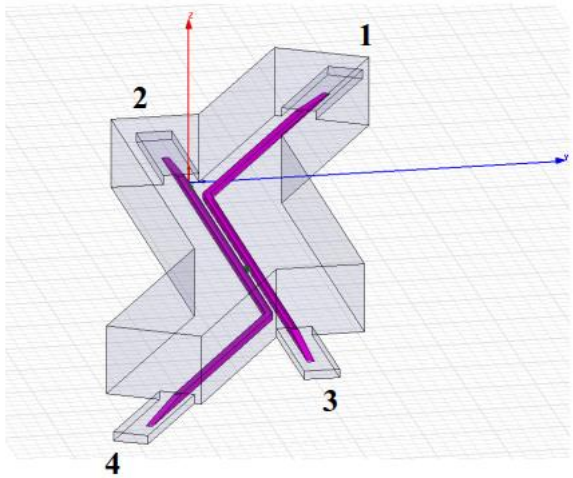

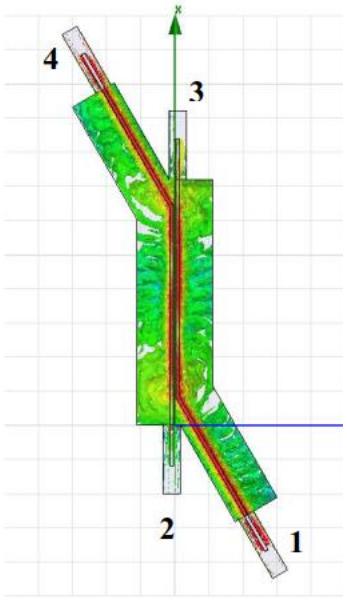

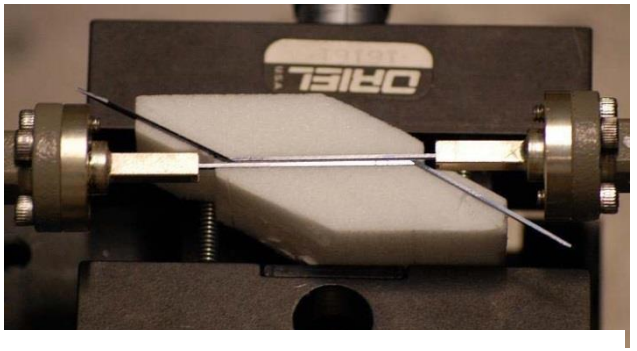

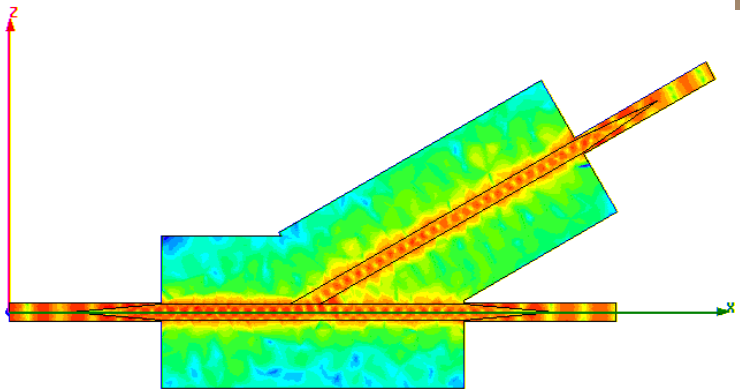

J. P. Pousi, S. N. Dudorov, D.V. Lioubtchenko, A. V. Räisänen, “Frequency selective coupler for W band based on power transfer in dielectric rod waveguides”, Proc. of the 4th European Conference of Antennas and Propagation (EuCAP10), Barcelona, Spain, 11-16 April, 2010

Mutual coupling between the sapphire rods with different vertical separation

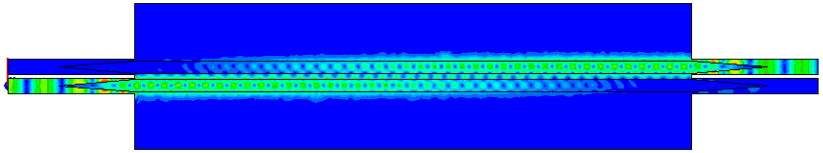

E field , 80 GHz, d=0.5 mm

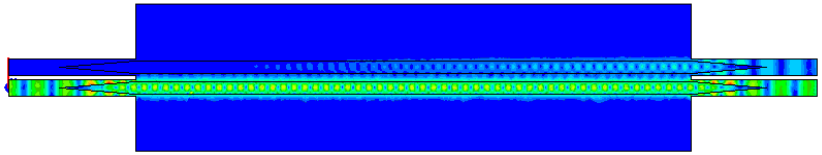

E field, 90 GHz, d=0.5 mm

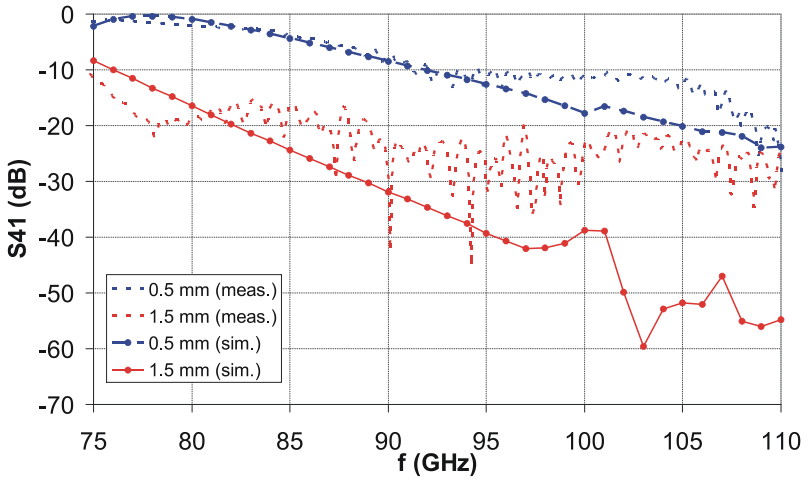

The S_{41} results are interesting and show that the coupling is very low when the distance is over 2.3 mm. With shorter distances the coupling is stronger and it seems that at some frequencies all the power is coupled to the upper rod. For example when the distance is 0.5 mm, S_{41} is -0.19 dB at 80 GHz. Simulated E field distributions are presented at 90 GHz and 80 GHz when the distance is 0.5 mm. It seems that the coupling is strongest at a rod length of 37-41λg. Phenomenon is similar to the crosstalk that can occur in optical fibers, where this complete power transfer is used e.g. in directional couplers. This phenomenon will be studied in more detail in the next section.

A mechanically controlled phase shifter

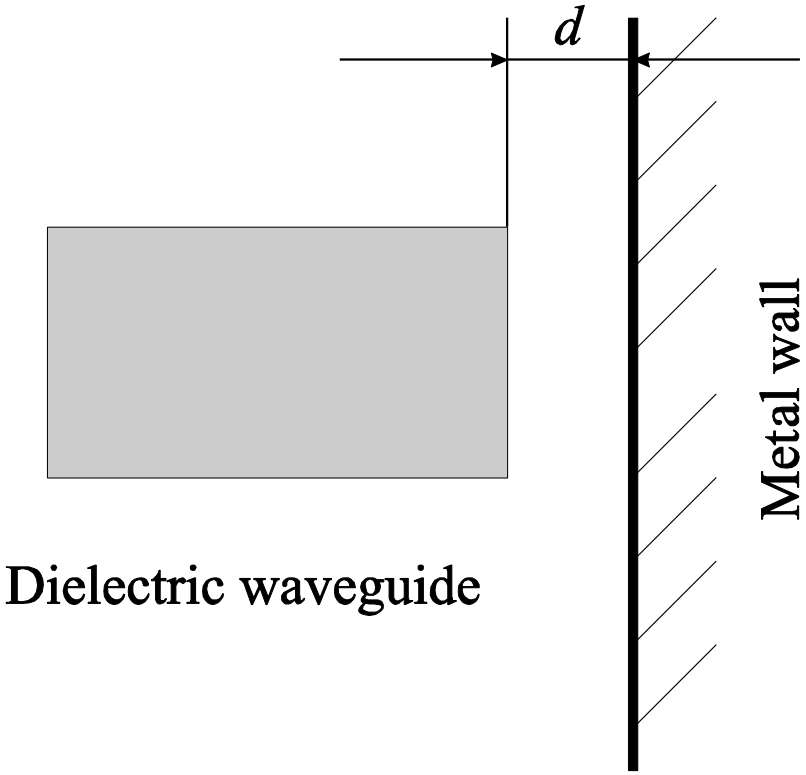

By introducing perturbation near the open DRW

Changing *d* results in the changing of the propagation constant, thus control the phase

MEMS based phase shifter

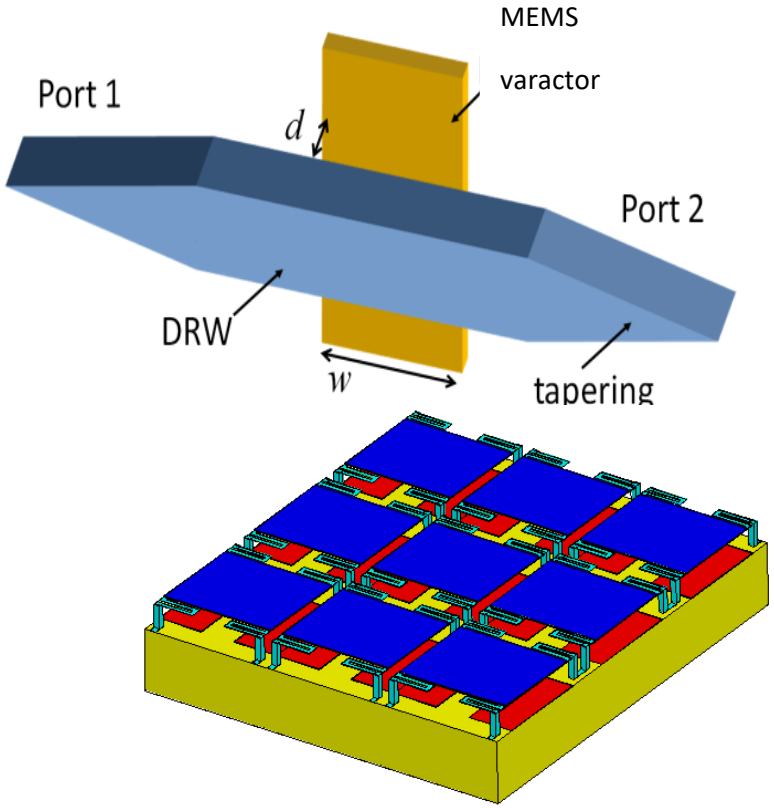

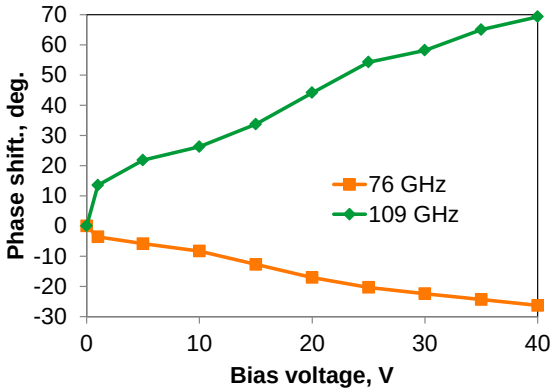

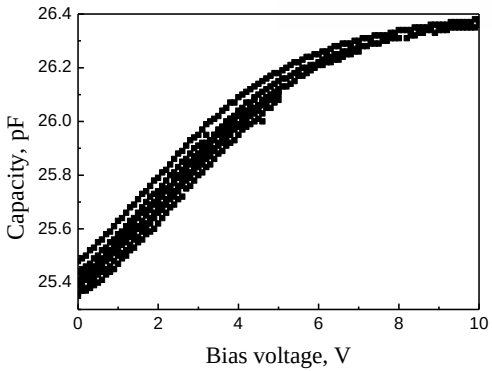

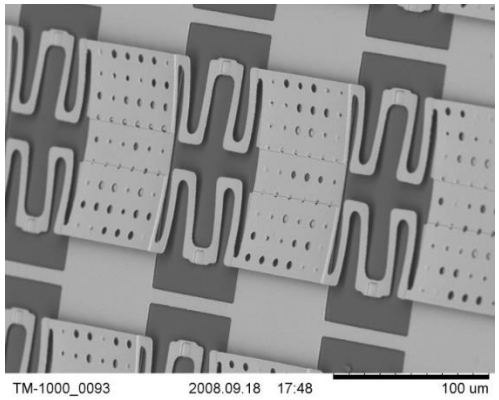

D. Chicherin, S. Dudorov, D. Lioubtchenko, V. Ovchinnikov, S. Tretyakov, A.V. Räisänen, "MEMS-based high-impedance surfaces for millimetre and submillimetre wave applications", Microwave and Optical Technology Letters, vol. 48, no. 12, 2006, p 2570-2573

Suspended carbon nanotubes MEMS

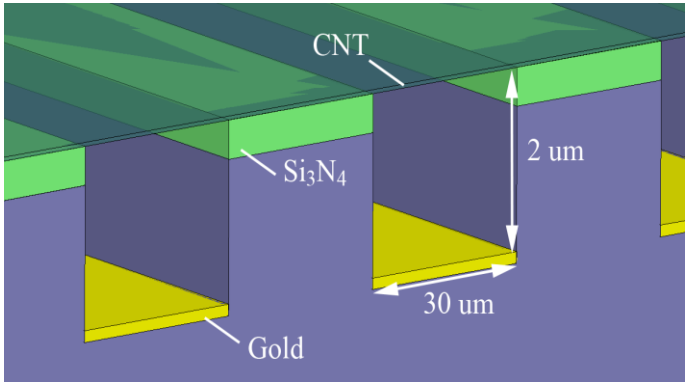

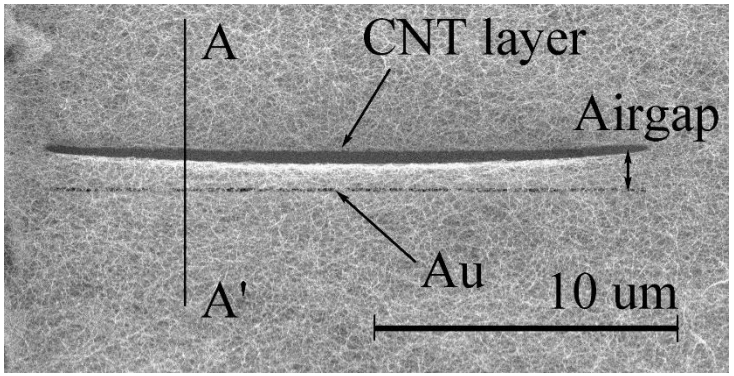

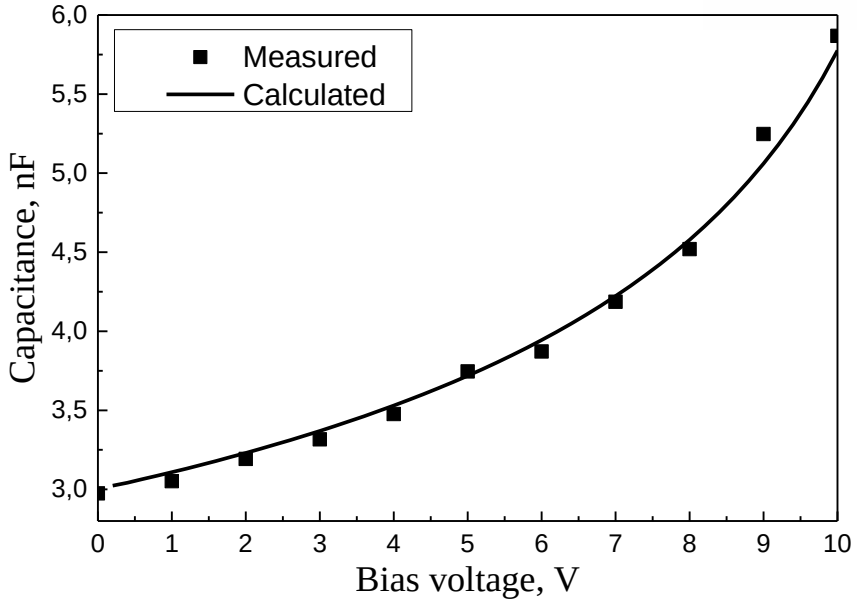

-higher tenability
-lower actuation voltage-
-require less fabrication steps
-100% tunability

A.A. Generalov, I.V. Anoshkin, M. Erdmanis, D.V. Lioubtchenko, V. Ovchinnikov, A.G. Nasibulin, and A V Räisänen, “Carbon nanotube network varactor” Nanotechnology vol. 26, no. 4, 2015 045201 (5pp).

Optically controlled silicon waveguide

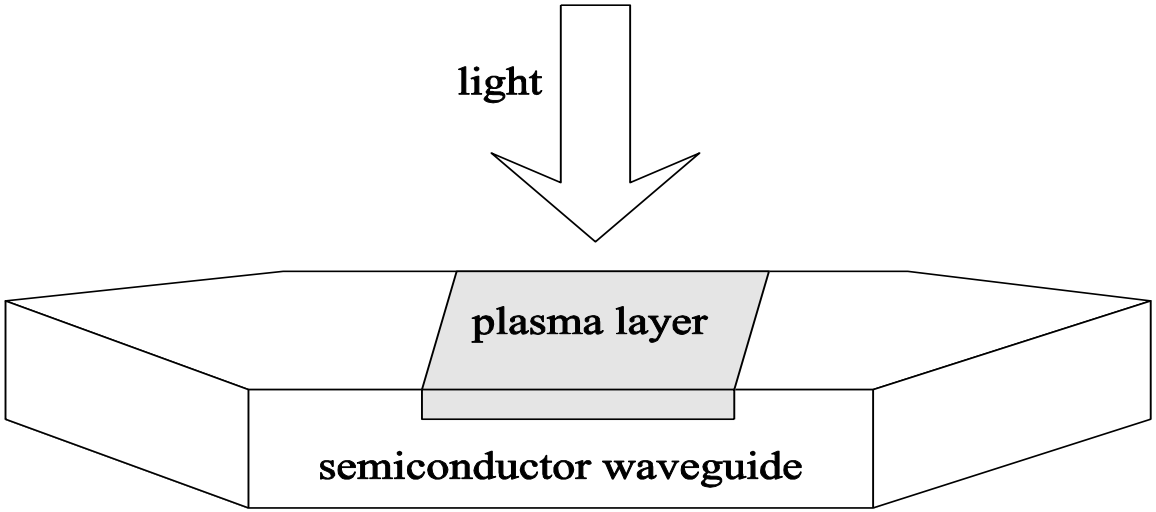

Optical control is realized by external light illumination of the broad side of the DRW using the plasma injection phenomenon. It is somewhat equivalent to placing metal to the surface of the DRW.

e.g. 30 ps pulses, a 0.53 μm wavelength with 50 μJ energy results in a 0.5 μm conducting layer appearance

Attenuation can be achieved by applying a longer wave of 1.03 μm (increasing the bulk conductivity)

Advantage – very fast response

CV measurements of CNTs

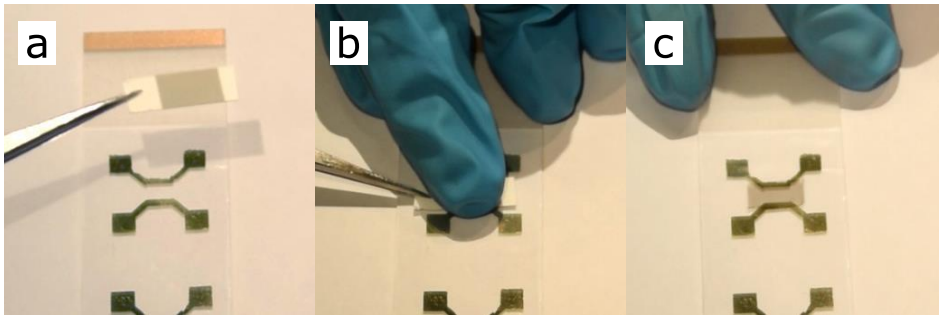

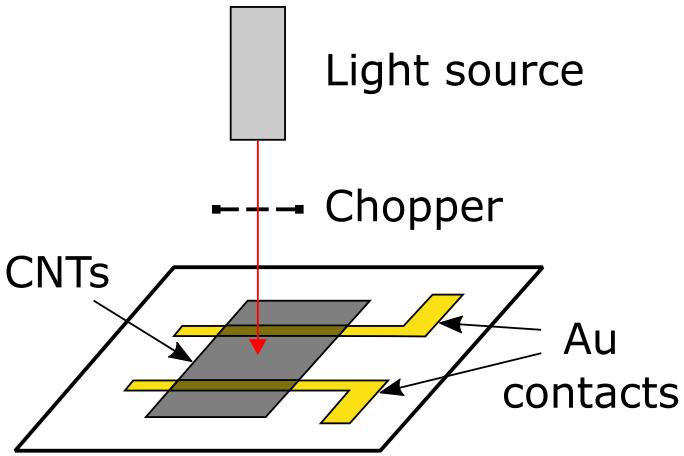

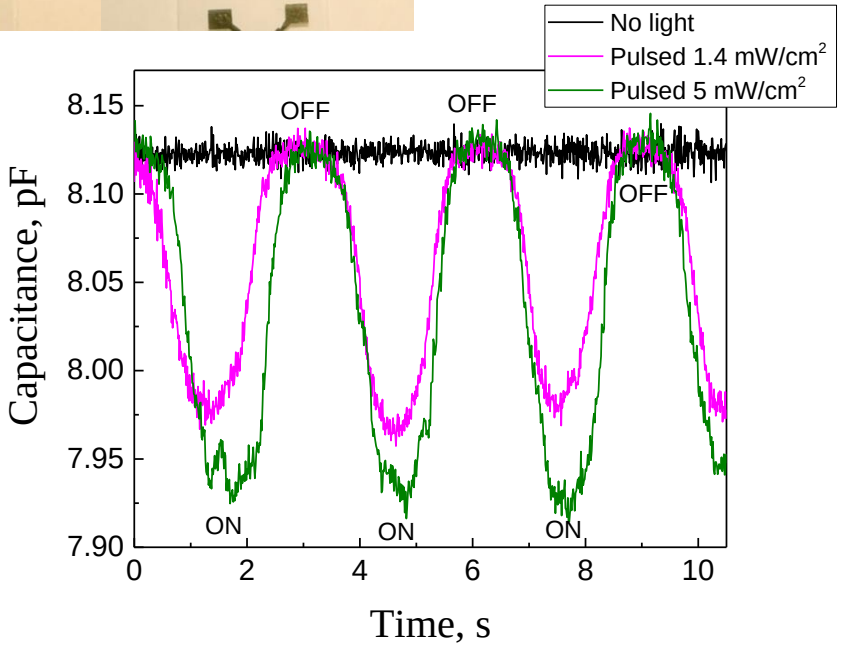

D.V. Lioubtchenko, I. Anoshkin, I.I. Nefedova, J. Oberhammer, and A. V. Räisänen, "W-band Phase Shifter Based on the Optimized Optically Controlled Carbon Nanotube Layer", *2017 IEEE MTT-S Int. Microwave Symp. (IMS)*, Honolulu, HI, 2017, pp. 1188-1191

CNT-based optically-controlled phase shifter

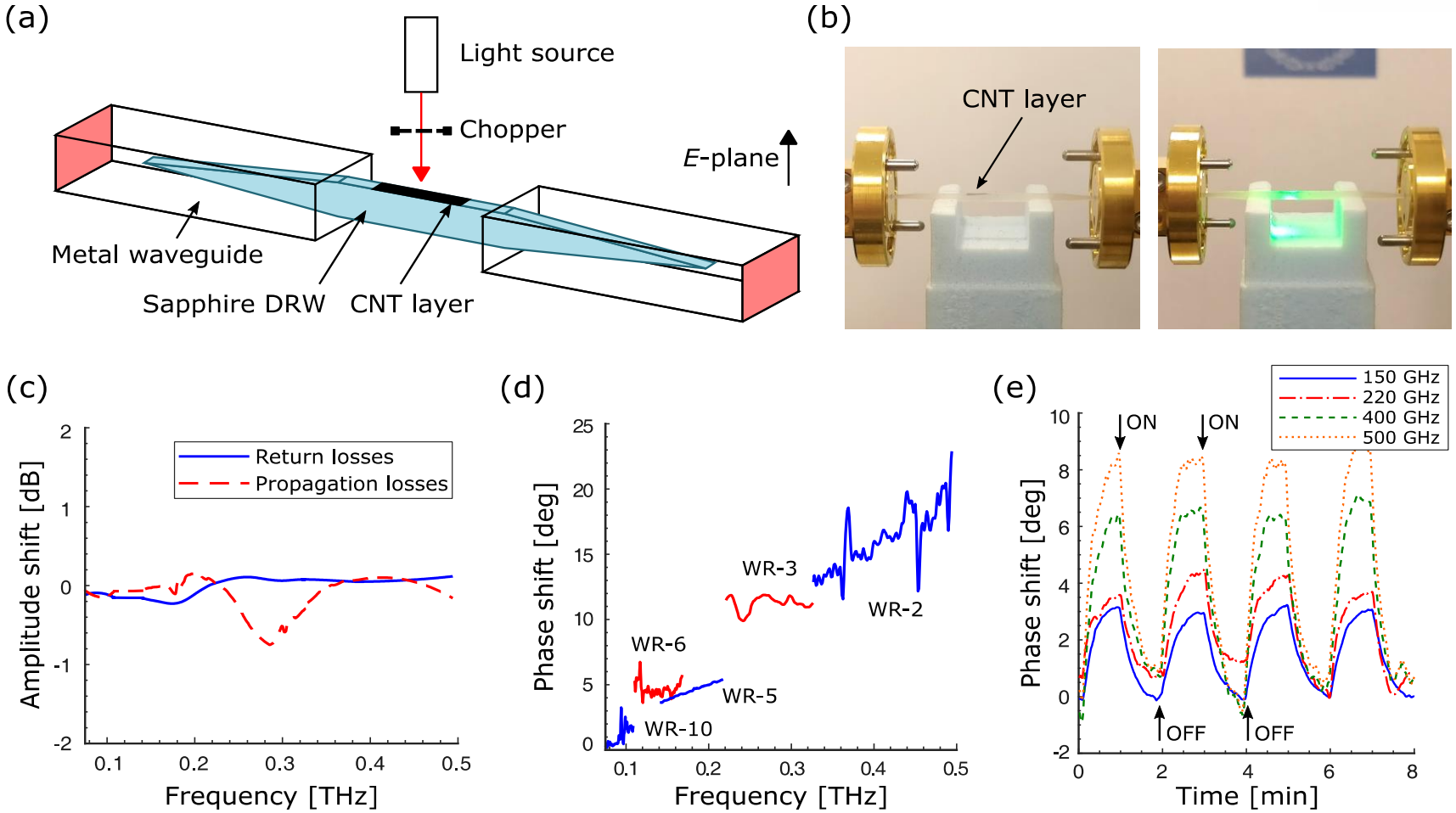

S. Smirnov, I.V. Anoshkin, P. Demchenko, D. Gomon, D.V. Lioubtchenko, M. Khodzitsky, J. Oberhammer, "Optically controlled dielectric properties of single-walled carbon nanotubes for terahertz wave applications", *Nanoscale*, vol. 10, is. 26, 2016, pp. 12291-12296.

Power sensor based on Si DRW

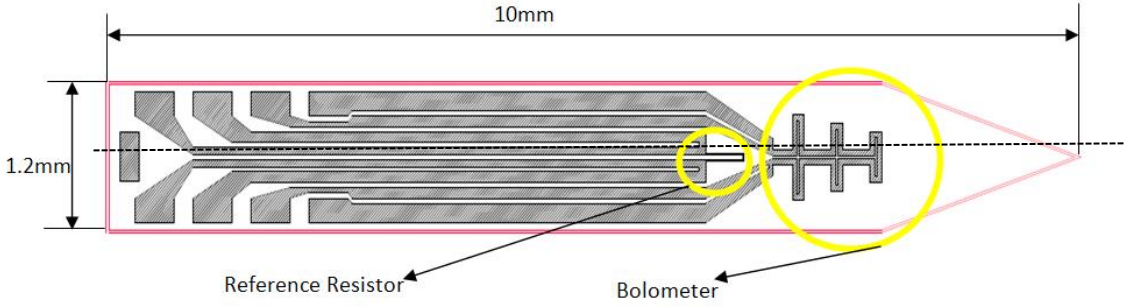

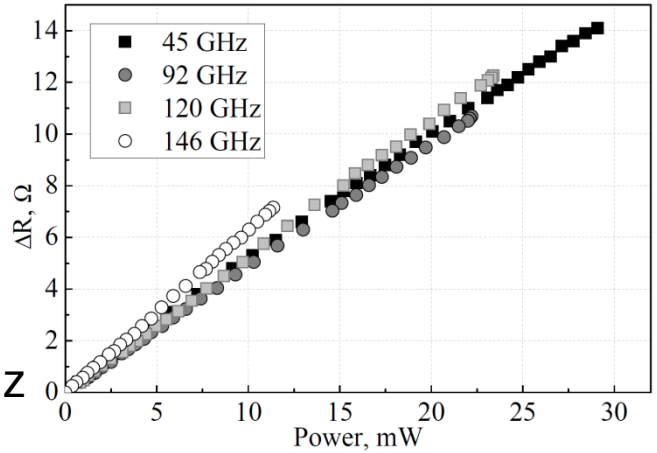

magnetron power source at 94 GHz

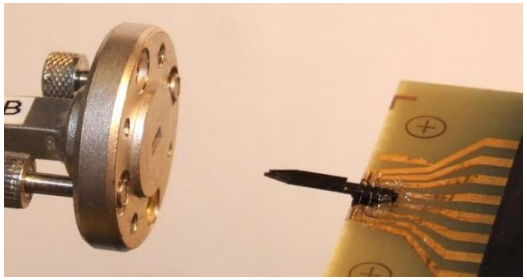

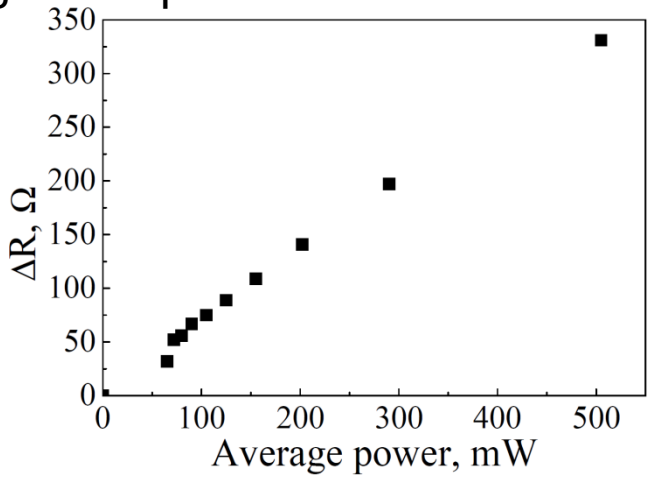

Gunn oscillator

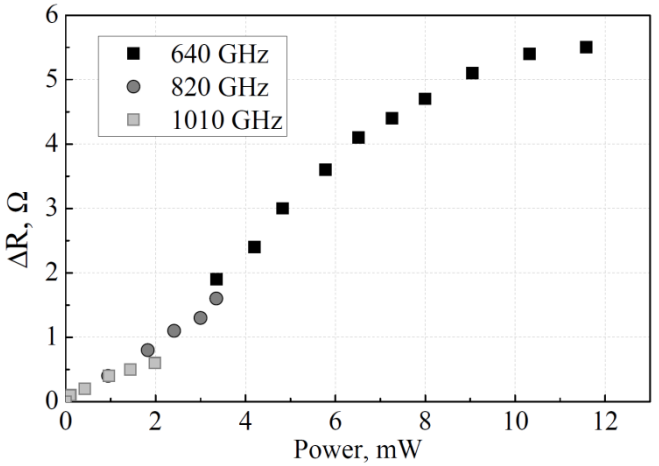

BWO

A.A. Generalov, D.V. Lioubtchenko, J.A. Mallat, V. Ovchinnikov, A.V. Räisänen, “Mm-wave Power Sensor Based on Silicon Rod Waveguide”, IEEE Trans. Terahertz Sci. Tech. v2, 2012, pp.623-628

Ultra wide-band DRW antenna

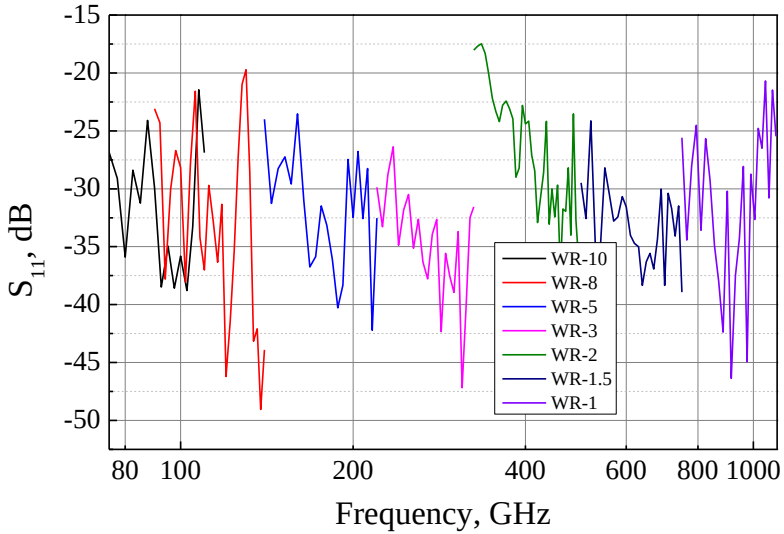

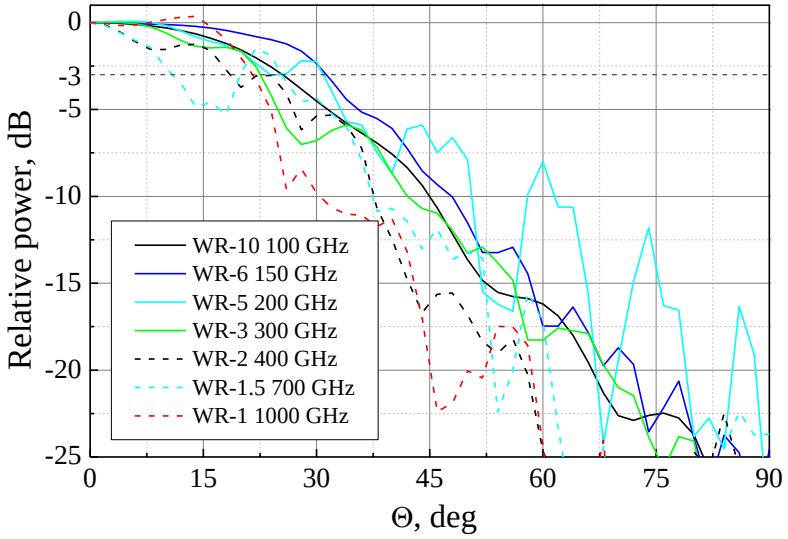

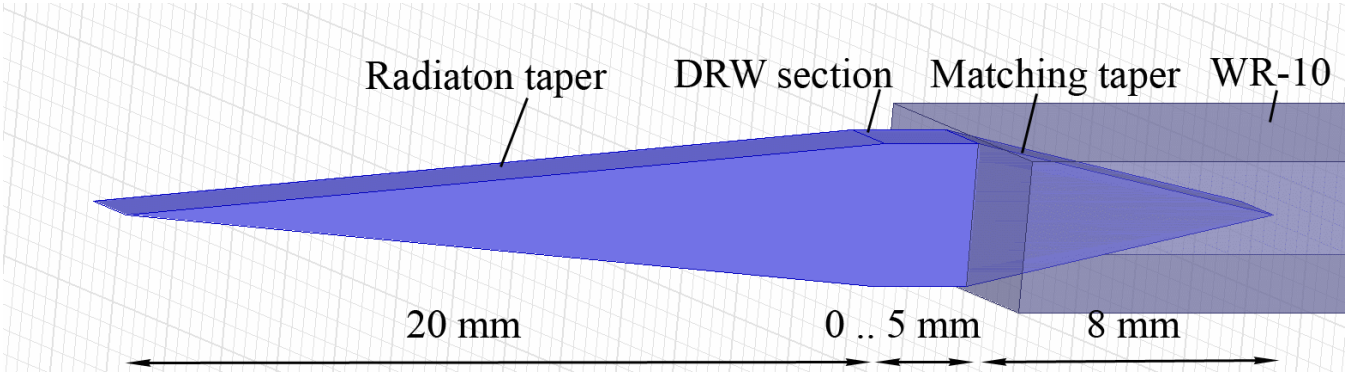

A.A. Generalov, J.A. Haimakainen, D.V. Lioubtchenko, and A.V. Räisänen, "Wide Band mm- and Submm-Wave Dielectric Rod Waveguide Antenna", *IEEE Trans. THz Sci. Technol.*, vol. 4, no 5, 2014, pp.568-574

Optically-controlled beam steering

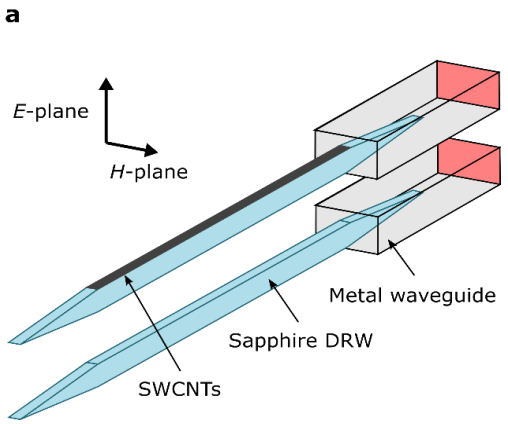

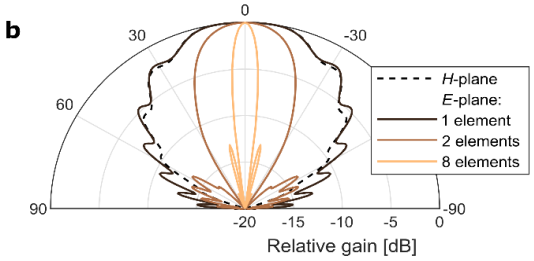

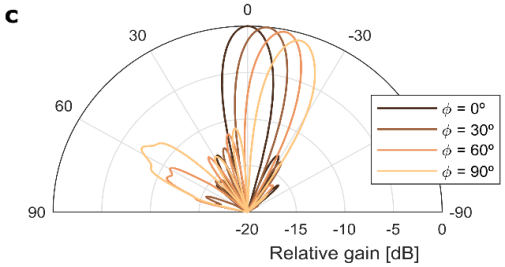

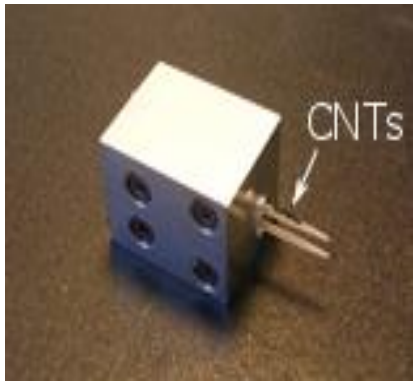

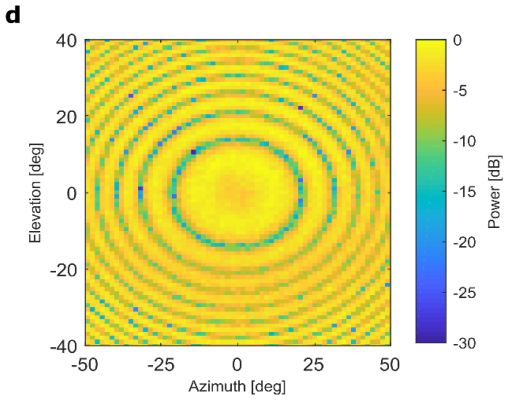

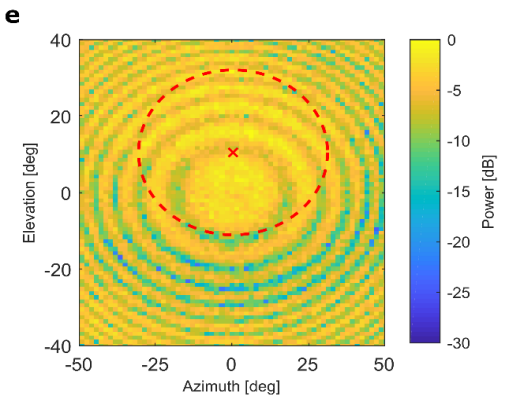

S. Smirnov, D. Lioubtchenko, J. Oberhammer "Single-walled carbon nanotube layers for millimeter-wave beam steering" *Nanoscale*, 2019, DOI: 10.1039/C9NR02705J

Antenna array with different CNT geometry

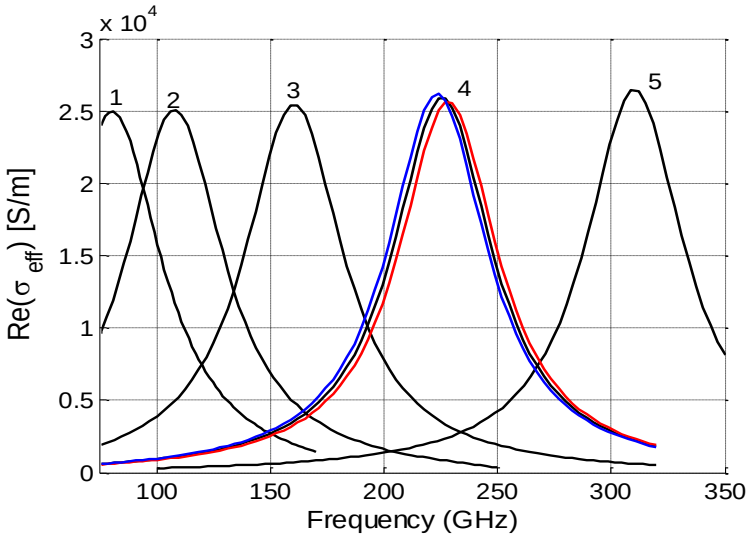

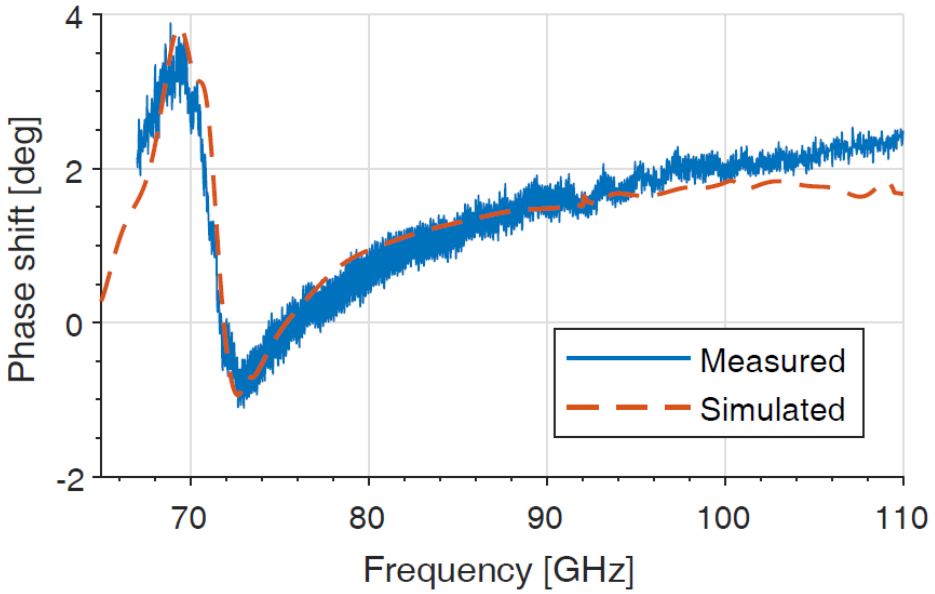

Sample	1	2	3	4	5
L (μm)	40	30	20	14	10
R (nm)				0.578 0.705 0.822	

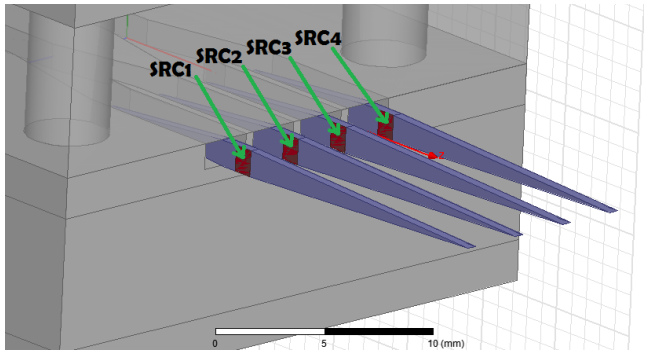

I.I. Nefedova, D.V. Lioubtchenko, I.S. Nefedov, and A.V. Räisänen "Carbon Nanotube Layers at Low Terahertz Frequencies" IEEE Transactions on Terahertz Science and Technology, vol. 6, is. 6, Nov. 2016, pp. 840-845

4 x 4 antenna array

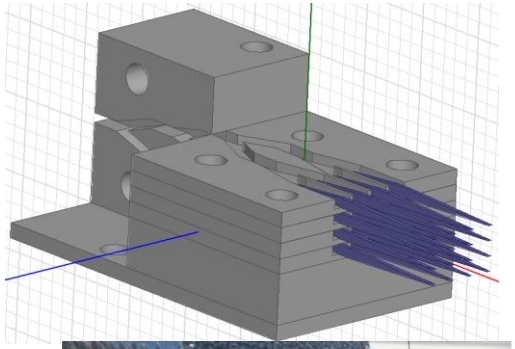

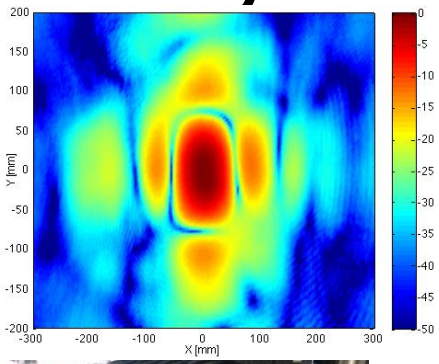

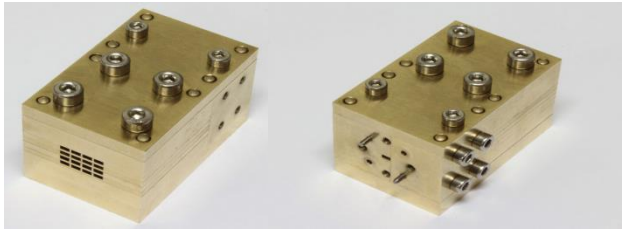

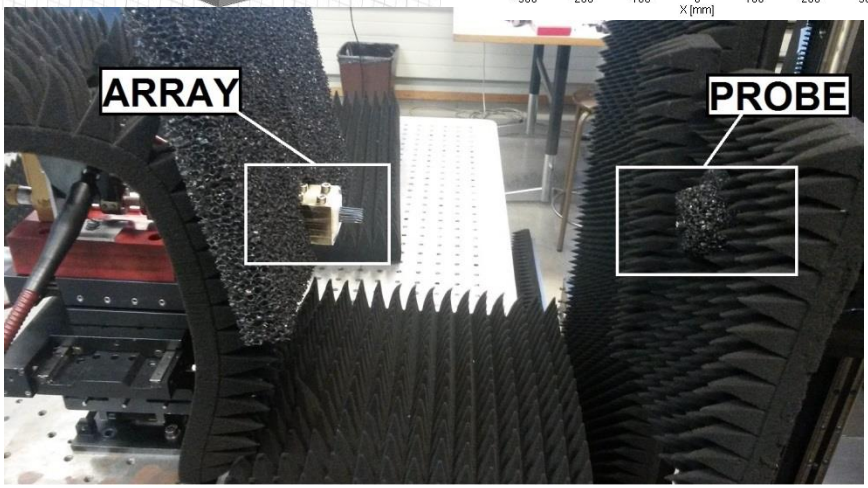

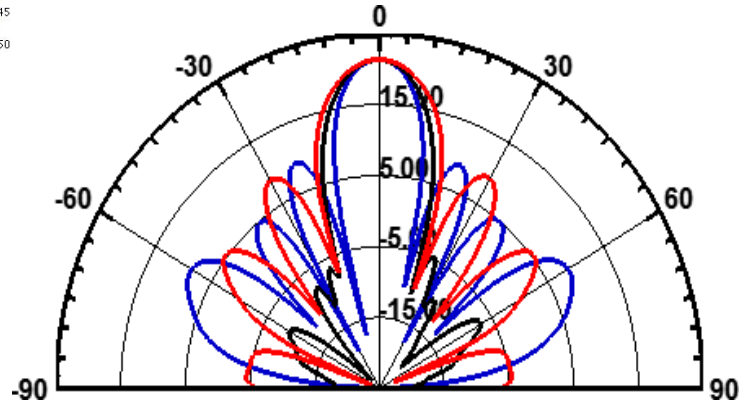

@ 100 GHz. Cuts ϕ=0º (red), ϕ=45º (black) and ϕ=90º (blue).

A. Rivera-Lavado, S. Preu, L.E. García-Muñoz, A. Generalov, J. Montero-de-Paz, G. Döhler, D. Lioubtchenko, M. Méndez-Aller, S. Malzer, D. Segovia-Vargas, A.V. Räisänen "Array of Dielectric Rod Waveguide Antennas for Millimeter-Wave Power Generation", *EuMC* 2015

Active DRW at puls regime

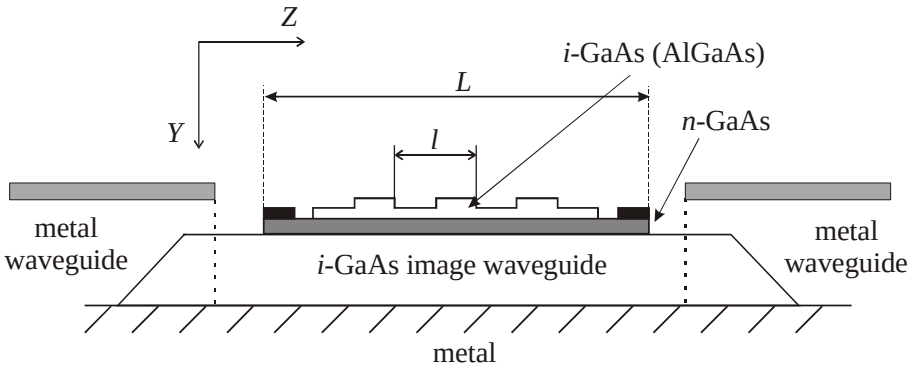

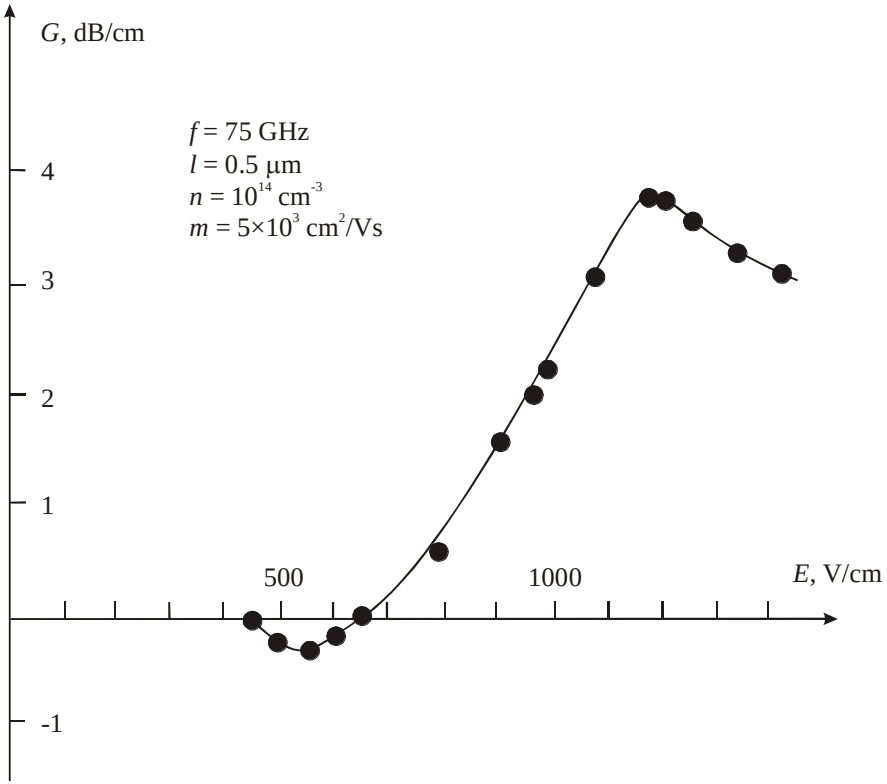

The condition for the first harmonic is given by

$$V_d > V_{ph} = \frac{\omega}{\beta_0 + 2\pi/l} \approx \frac{\omega}{2\pi/l} = c\frac{l}{\lambda_0},$$

V.E. Lyubchenko, V.A. Martyakhin, "Travelling wave amplification in GaAs image waveguide at V-band", Electronic Letters, vol. 30, no. 11, 1994, pp. 869-870

Active DRW

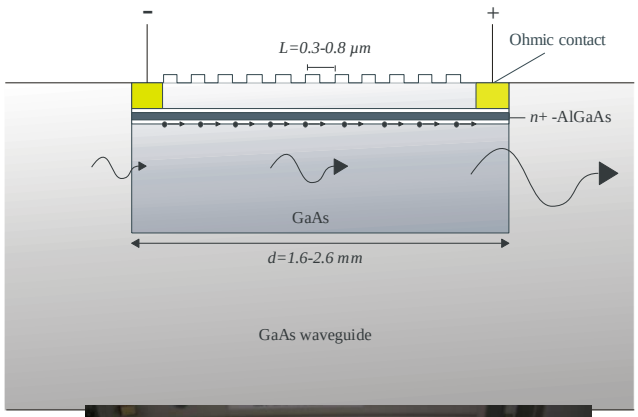

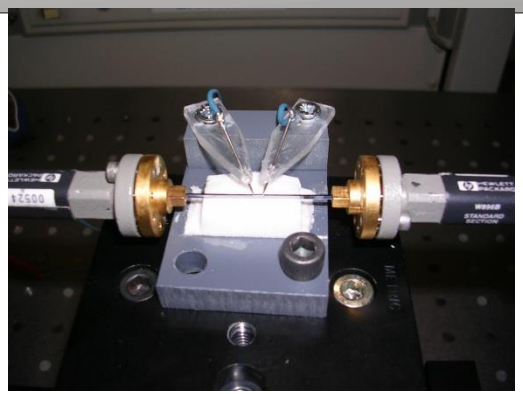

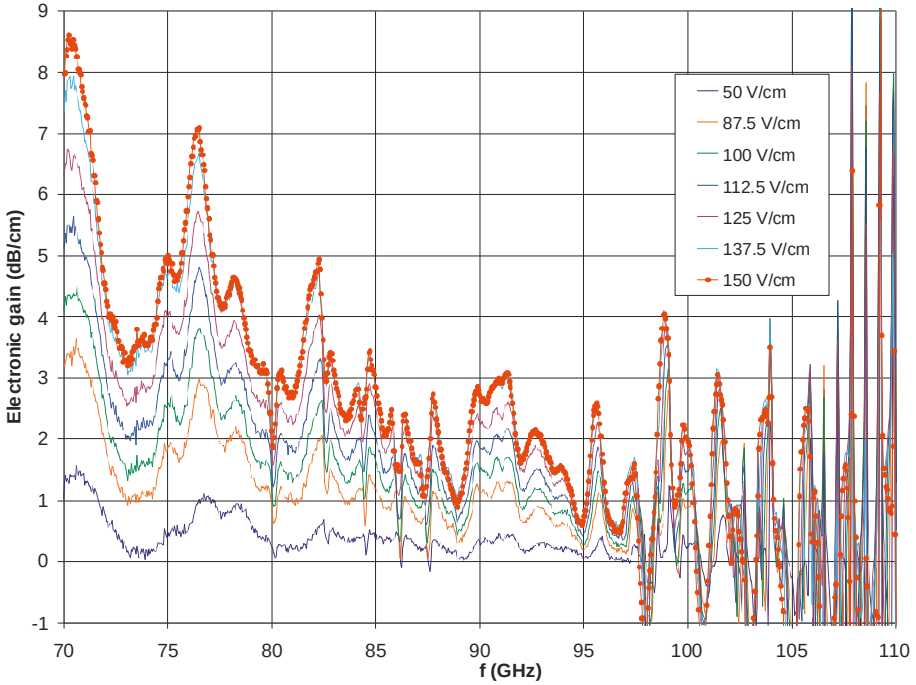

P. Pousi, D. Lioubtchenko, S. Dudorov, A.V. Räisänen, “Dielectric rod waveguide travelling wave amplifier based on AlGaAs/GaAs heterostructure”, Proc. EuMC, 2008, pp. 1082-1085

DRW combined with photomixer

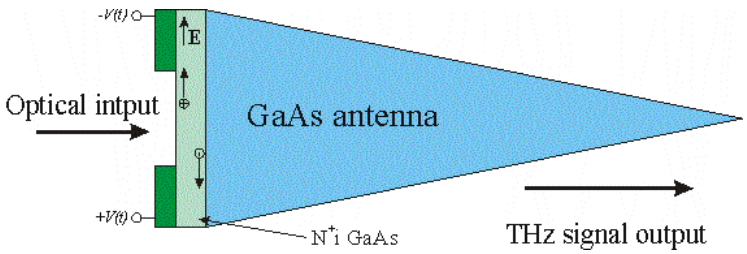

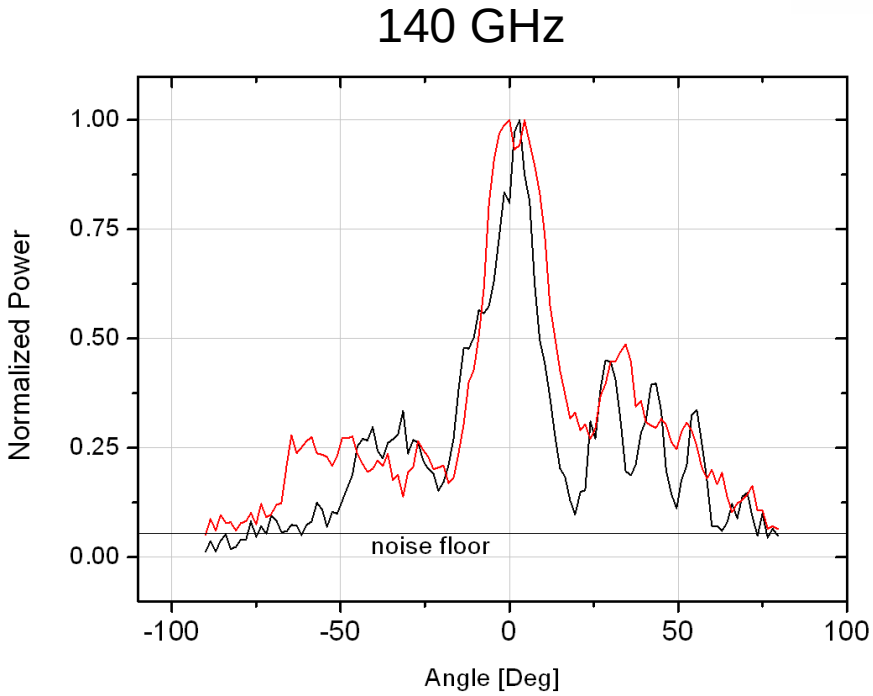

A. Rivera-Lavado, S. Preu, L.E. García-Muñoz, A. Generalov, J. Montero-de-Paz, G. Döhler, D. Lioubtchenko, M. Méndez-Aller, F. Sedlmeir, M. Schneidereit, H.G.L. Schwefel, S. Malzer, D. Segovia-Vargas, and A.V. Räisänen, "Dielectric rod waveguide antenna as THz emitter for photomixing devices", IEEE Transactions on Antenna and Propagation vol. 63, 2015, pp. 1-9

4 x 4 antenna array

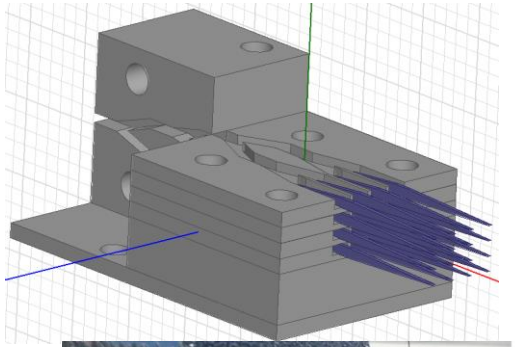

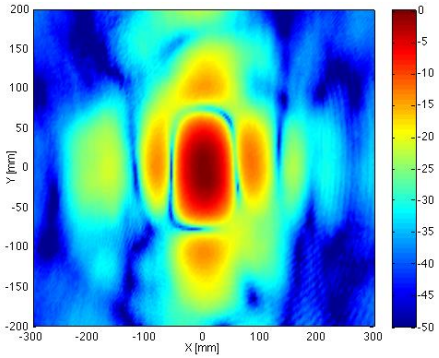

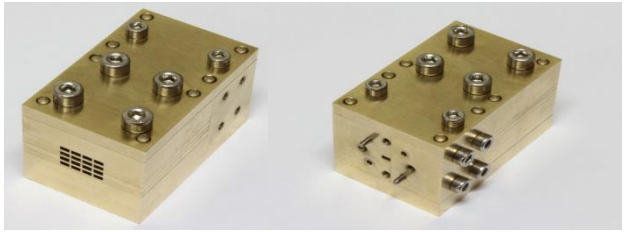

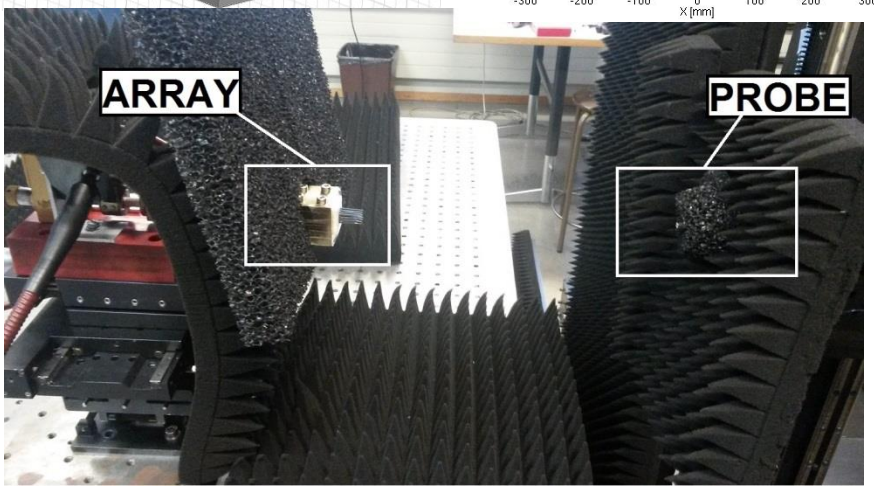

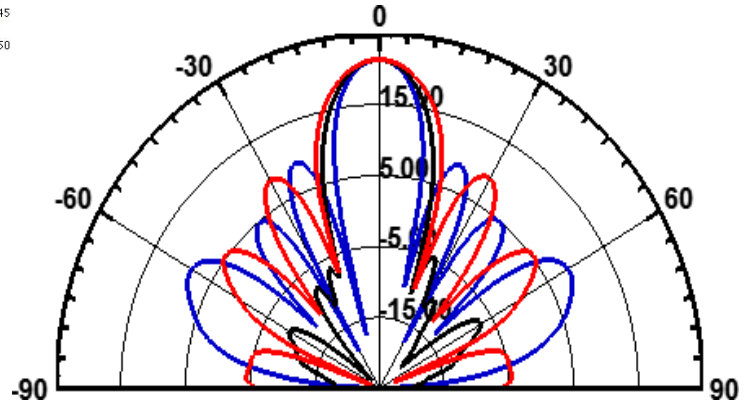

@ 100 GHz. Cuts ϕ=0º (red), ϕ=45º (black) and ϕ=90º (blue).

A. Rivera-Lavado, S. Preu, L.E. García-Muñoz, A. Generalov, J. Montero-de-Paz, G. Döhler, D. Lioubtchenko, M. Méndez-Aller, S. Malzer, D. Segovia-Vargas, A.V. Räisänen “Array of Dielectric Rod Waveguide Antennas for Millimeter-Wave Power Generation”, EuMC 2015

Photomixers combined with phase shifter and travelling wave amplifier on DRW

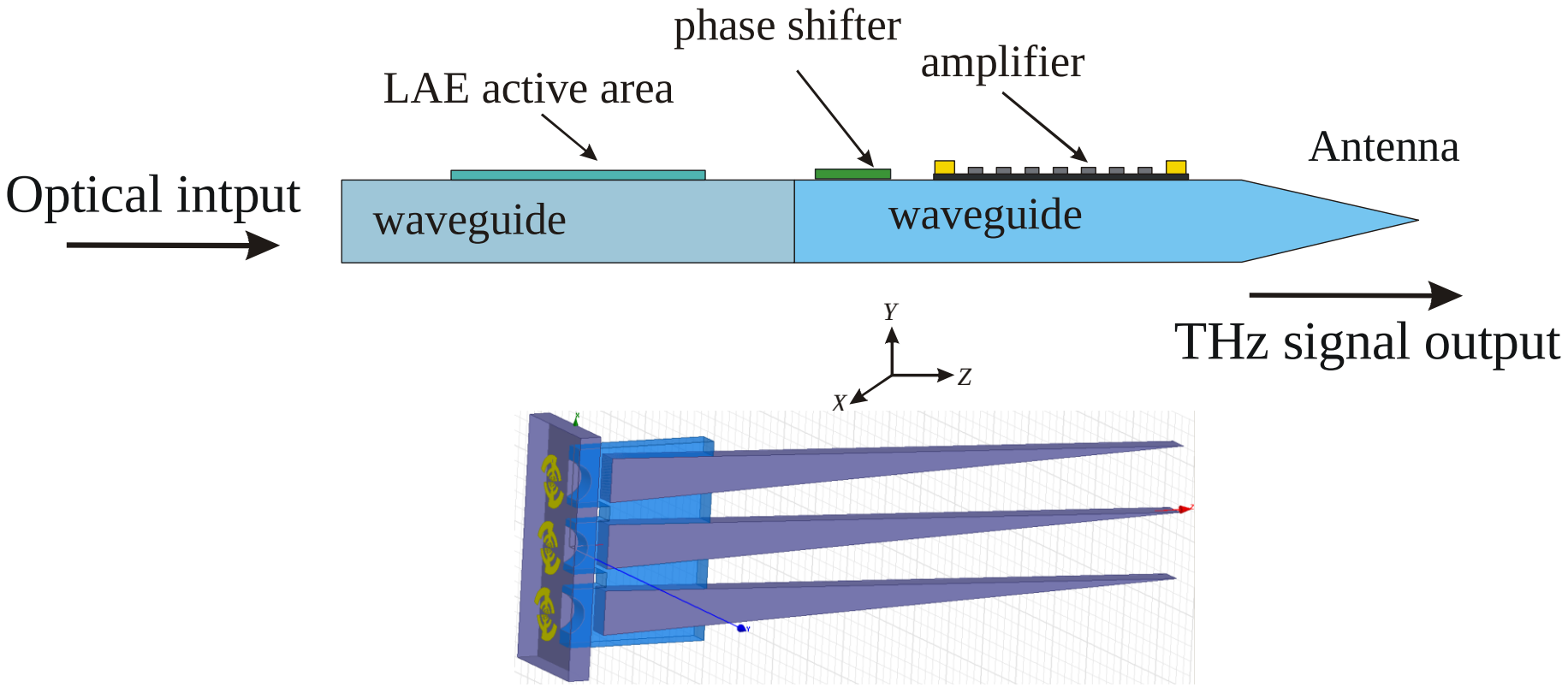

DRW for dielectric constant measurements

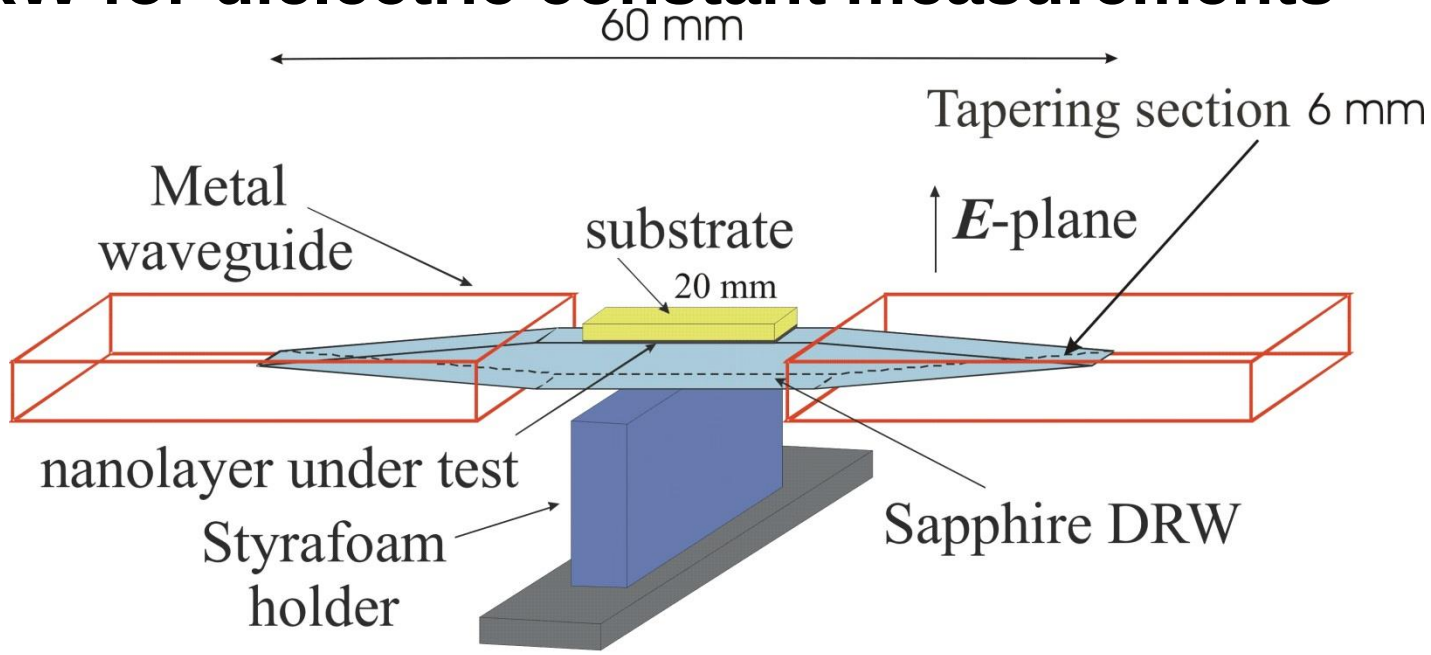

HFSS simulations

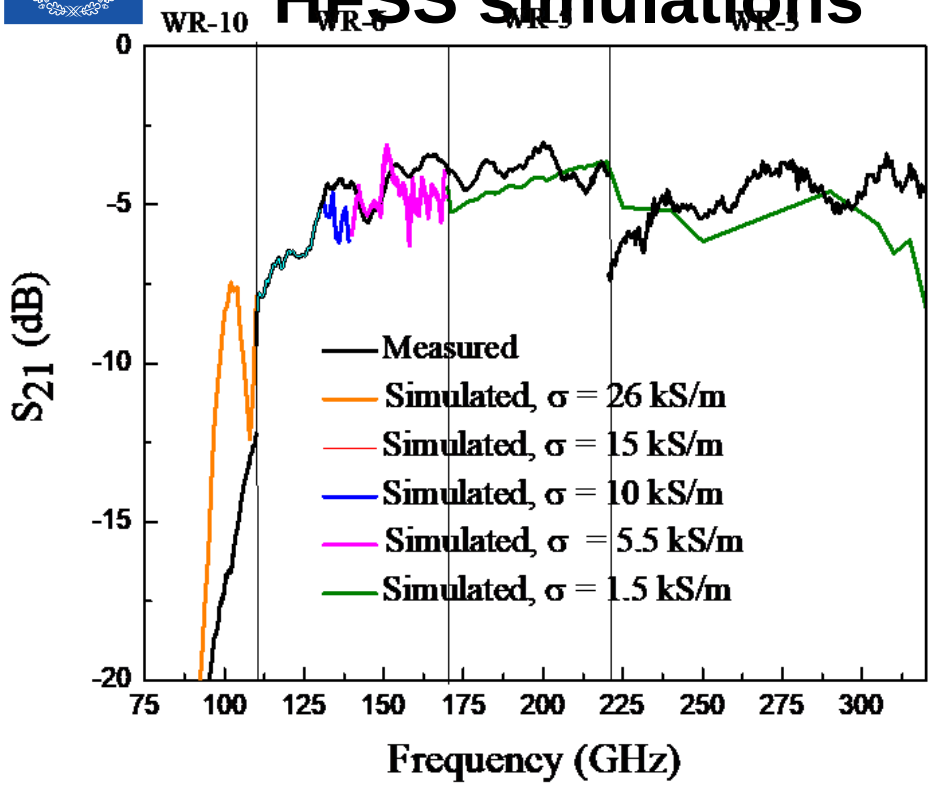

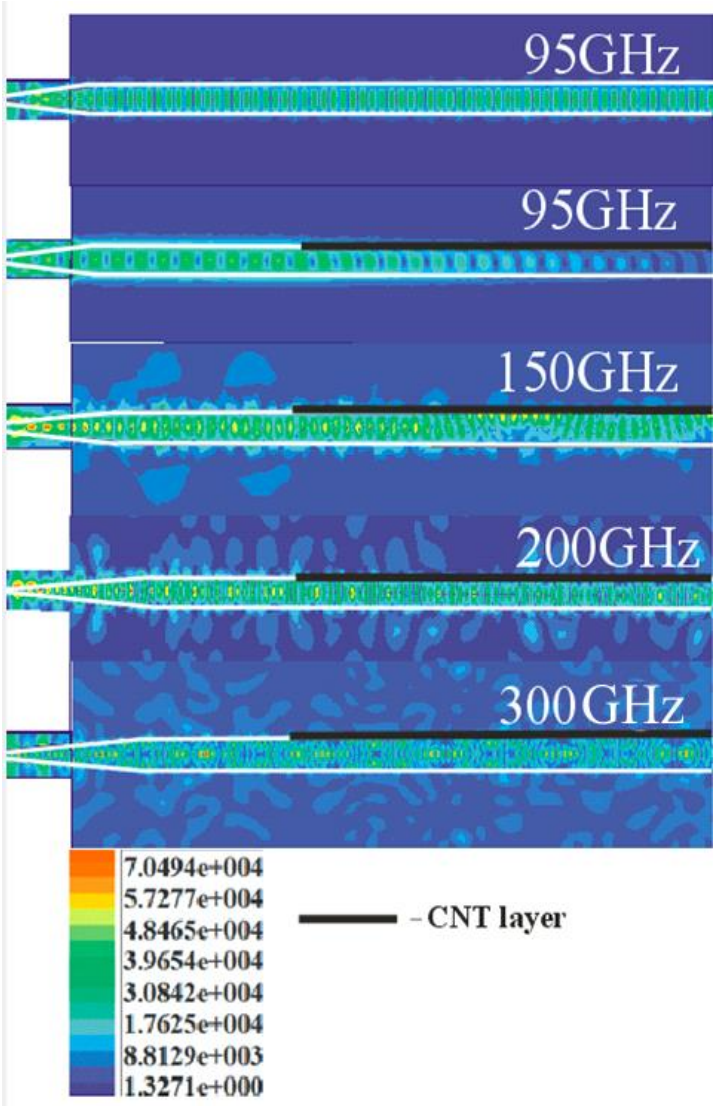

I.I. Nefedova, D.V. Lioubtchenko, I.S. Nefedov, and A.V. Räisänen "Carbon Nanotube Layers at Low Terahertz Frequencies" accepted to IEEE Transactions on Terahertz Science and Technology

Simulations of AgNws

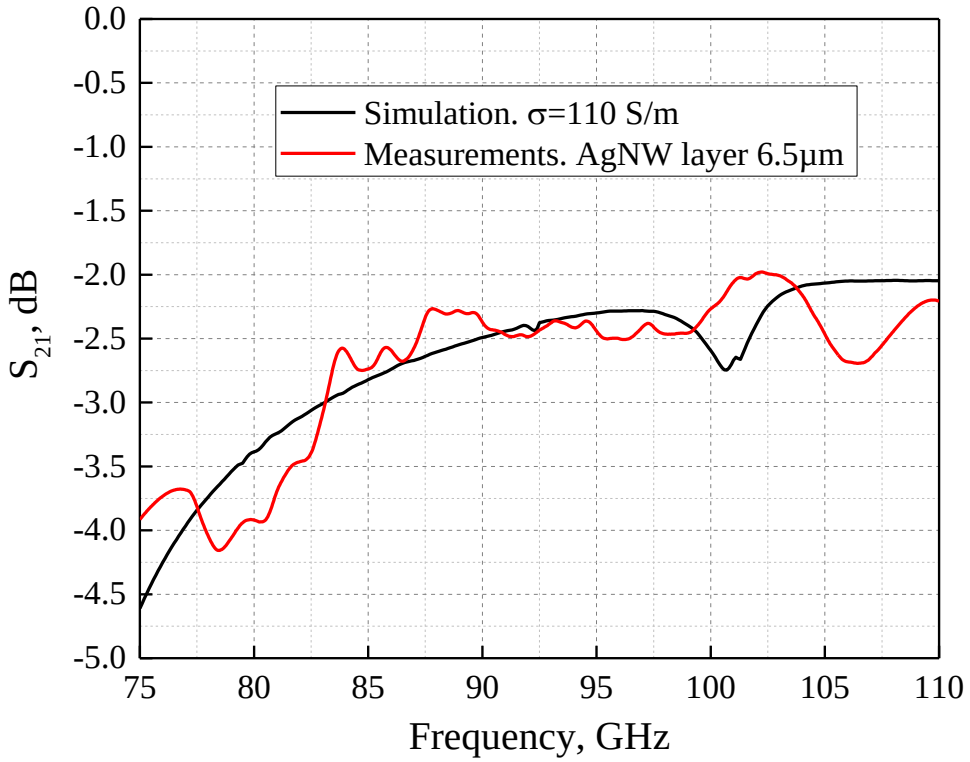

I. Nefedova, D.V. Lioubtchenko, I. Nefedov, I. Anoshkin, and A. V. Räisänen, “Millimeter waves conductivity of silver nanowires”, GSMM Global Symposium on Millimeter-Waves 2016, Espoo, Finland, June 6-8, 2016

HFSS simulations

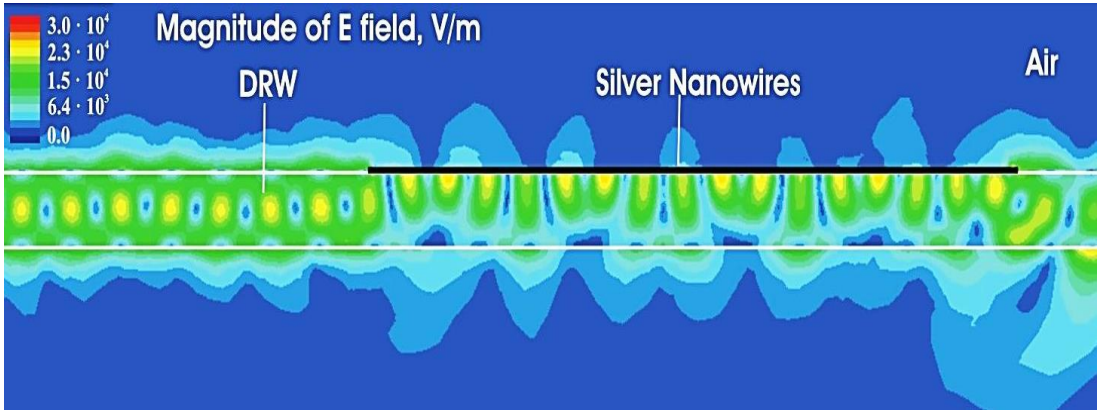

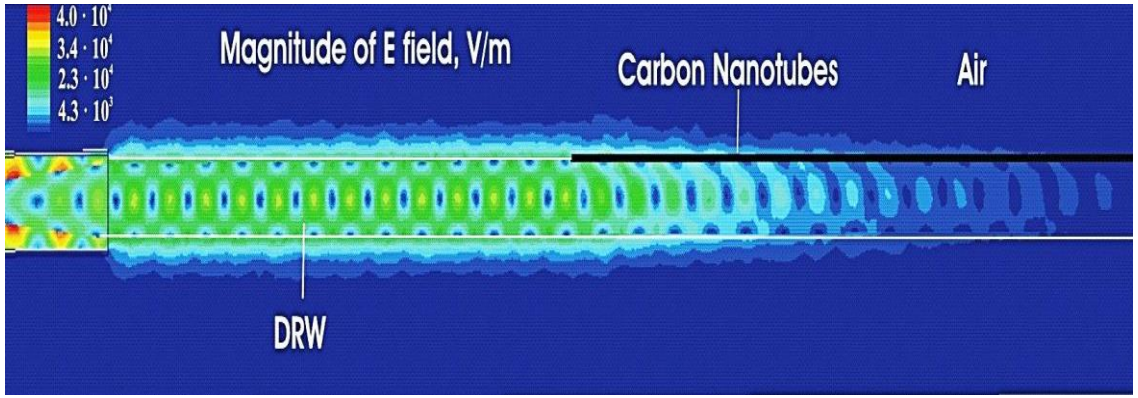

I. Nefedova, D.V. Lioubtchenko, I. Nefedov, I. Anoshkin, and A. V. Räisänen, “Millimeter waves conductivity of silver nanowires”, GSMM Global Symposium on Millimeter-Waves 2016, Espoo, Finland, June 6-8, 2016

Conclusions

- DRW is a prospective novel platform for future ultra-wide band THz telecommunication systems.
- Compatibility with standard Si and GaAs/InP technologies as well as with novel nanomaterials offers new opportunities for the passive and active devices and integrated circuits.
- Up-to-date some devices based on DRWs are already developed and used.